

PB 278 034

REPORT NO. FRA/ORD-77/51

**STRUCTURAL ADEQUACY OF FREIGHT
CAR TRUCK CASTINGS AND WHEELS**

Milton R. Johnson

IIT Research Institute
10 West 35th Street
Chicago IL 60616



OCTOBER 1977
FINAL REPORT

DOCUMENT IS AVAILABLE TO THE U.S. PUBLIC
THROUGH THE NATIONAL TECHNICAL
INFORMATION SERVICE, SPRINGFIELD,
VIRGINIA 22161

Prepared for
U.S. DEPARTMENT OF TRANSPORTATION
FEDERAL RAILROAD ADMINISTRATION
Office of Research and Development
Washington DC 20590

REPRODUCED BY
**NATIONAL TECHNICAL
INFORMATION SERVICE**
U.S. DEPARTMENT OF COMMERCE
SPRINGFIELD, VA. 22161

NOTICE

This document is disseminated under the sponsorship of the Department of Transportation in the interest of information exchange. The United States Government assumes no liability for its contents or use thereof.

NOTICE

The United States Government does not endorse products or manufacturers. Trade or manufacturers' names appear herein solely because they are considered essential to the object of this report.

Technical Report Documentation Page

1. Report No. FRA/ORD-77/ 51		2. Government Accession No.		3. Recipient's Catalog No. PB278034	
4. Title and Subtitle STRUCTURAL ADEQUACY OF FREIGHT CAR TRUCK CASTINGS AND WHEELS				5. Report Date October 1977	
7. Author(s) Milton R. Johnson				6. Performing Organization Code	
9. Performing Organization Name and Address IIT Research Institute* 10 West 35th Street Chicago IL 60616				8. Performing Organization Report No. DOT-TSC-FRA-77-18	
12. Sponsoring Agency Name and Address U.S. Department of Transportation Federal Railroad Administration Office of Research and Development Washington DC 20590				10. Work Unit No. (TRAIS) RR828/R8327	
				11. Contract or Grant No. DOT-TSC-727	
				13. Type of Report and Period Covered Final Report (Apr. 1976-Nov. 1976)	
				14. Sponsoring Agency Code	
15. Supplementary Notes * Under contract to: U.S. Department of Transportation Transportation Systems Center Kendall Square Cambridge MA 02142					
16. Abstract The structural adequacy of freight car truck castings and wheels to resist fatigue damage is reviewed. The environmental load data described in an earlier report under this program and additional load data which have only recently become available are used to calculate the expected fatigue life under various assumptions of the stresses present in the components. It is found that under most conditions the components should not develop fatigue cracks. This confirms the observation that there are a relatively small number of fatigue failures of these components in service. Since failures of these components can lead to serious derailments, it is important that the circumstances leading to a higher risk of fatigue failure be identified so that under these circumstances truck components can be subjected to more frequent and stringent inspections under the railroad freight car safety standards of the FRA. The results of tests to determine the fatigue strength of wheel plates are also described. The tests showed that there is a substantial safety margin with respect to fatigue when one considers the effects of lateral loads acting on the wheel.					
17. Key Words Fatigue Analysis, Railroad Truck Side Frames, Railroad Truck Bolsters, Railroad Wheels.			18. Distribution Statement DOCUMENT IS AVAILABLE TO THE U.S. PUBLIC THROUGH THE NATIONAL TECHNICAL INFORMATION SERVICE, SPRINGFIELD, VIRGINIA 22161		
19. Security Classif. (of this report) Unclassified		20. Security Classif. (of this page) Unclassified		21. No. of Pages 82	22. Price PC-A05 MF-AD1

PREFACE

This report presents final results obtained under the Department of Transportation, Transportation Systems Center (TSC) Contract DOT-TSC-727 titled "Analysis of Railroad Car Truck and Wheel Fatigue". This project, which has been conducted under the overall sponsorship of the Federal Railroad Administration, was initiated in June 1972. It has been conducted by IIT Research Institute under the direction of Dr. Milton R. Johnson, Project Manager.


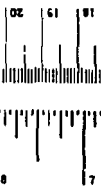
The wheel plate fatigue tests described in this report were conducted by the Research and Tests Laboratory of the Southern Railway System under the direction of Mr. D. J. Reynolds, Assistant Manager Research and Tests, Mechanical. The data included in this report from the Railway Progress Institute/Association of American Railroads Truck Research Safety and Test Project were made available through Mr. R. Evans, Project Director. Mr. Roger Steele has served as the TSC technical project officer and his helpful comments and suggestions in guiding the course of the work are gratefully acknowledged.

This report is a review of the structural adequacy of freight car truck castings and wheels to resist fatigue damage and is based on results from analytical and experimental evaluations of the fatigue strengths of these components. Earlier reports have described the loads acting on these truck components under service conditions. Supplemental load data are also included in this report.

METRIC CONVERSION FACTORS

Approximate Conversions to Metric Measures		Approximate Conversions from Metric Measures		
Symbol	When You Know	Multiply by	To Find	Symbol
LENGTH				
in	inches	2.5	centimeters	cm
ft	feet	30	centimeters	cm
yd	yards	0.9	meters	m
mi	mi-ls	1.6	kilometers	km
AREA				
sq ft	square feet	0.09	square meters	m ²
sq yd	square yards	0.8	square meters	m ²
sq mi	square miles	2.6	square kilometers	km ²
acres	acres	0.4	hectares	ha
MASS (weight)				
oz	ounces	28	grams	g
lb	pounds	0.45	kilograms	kg
	short tons (2000 lb)	0.9	tonnes	t
VOLUME				
cup	cup	0.24	liters	l
fl oz	fluid ounces	0.07	liters	l
qt	quarts	0.95	liters	l
gal	gallons	3.8	liters	l
cu ft	cubic feet	0.03	cubic meters	m ³
cu yd	cubic yards	0.76	cubic meters	m ³
TEMPERATURE (exact)				
F	Fahrenheit temperature	$(F - 32) \times \frac{5}{9}$	Celsius temperature	C
C	Celsius temperature	$C \times \frac{9}{5} + 32$	Fahrenheit temperature	F

Approximate Conversions from Metric Measures	
When You Know	Multiply by
LENGTH	
millimeters	0.04
centimeters	0.4
meters	3.3
kilometers	0.6
AREA	
square centimeters	0.16
square meters	1.2
square kilometers	0.4
hectares (10,000 m ²)	2.5
MASS (weight)	
grams	0.035
kilograms	2.2
tonnes (1000 kg)	1.1
VOLUME	
milliliters	0.03
liters	2.1
liters	1.06
cubic meters	35
cubic meters	1.3
TEMPERATURE (exact)	
Celsius temperature	$C \times \frac{9}{5} + 32$
Fahrenheit temperature	$(F - 32) \times \frac{5}{9}$

CONTENTS

	<u>Page</u>
1. INTRODUCTION	1
1.1 Objectives	1
1.2 Background	1
1.2.1 Reliability Goals	1
1.2.2 Failure Rates	1
1.2.3 Safety Standards	3
2. TRUCK COMPONENT LOADS	5
2.1 Load Characteristics	5
2.1.1 Vertical Loads	5
2.1.2 Lateral Loads	8
2.1.3 Other Mechanical Loads	8
2.1.4 Wheel Thermal Loads	8
2.2 Magnitudes of Truck Component Loads	9
2.2.1 Summary of Earlier Project Test Data	9
2.2.2 Railway Progress Institute/Association of American Railroads Truck Project Data	11
2.2.3 Data from Tank Car Tests	14
3. FAILURE MODES	17
3.1 Truck Castings	17
3.1.1 Side Frames	17
3.1.2 Bolsters	18
3.2 Wheels	19
3.2.1 Radial Rim Cracks	19
3.2.2 Plate Cracks	20
3.2.3 Shattered Rim	21
4. DESIGN STRESSES AND THEIR RELATIONSHIP TO FATIGUE DAMAGE	22
4.1 Truck Castings	22
4.1.1 Material Properties	22
4.1.2 Side Frame Design Stresses	22
4.1.3 Bolster Design Stresses	24
4.2 Wheels	26
4.2.1 Material Properties	26
4.2.2 Design Stresses	26
4.3 Fatigue Evaluation	32
4.3.1 Side Frames	33
4.3.2 Bolsters	36
4.3.3 Wheels	37

CONTENTS (Concl)

	<u>Page</u>
5. FATIGUE TEST DATA	47
5.1 Side Frames	47
5.2 Wheel Fatigue Tests	48
5.2.1 Background	48
5.2.2 Test Procedures and Results	51
5.2.3 Interpretation of Wheel Plate Fatigue Tests	55
6. CONCLUSIONS AND RECOMMENDATIONS	57
7. REFERENCES	61
APPENDIX A - CALCULATION OF SIDE FRAME AND TRUCK BOLSTER FATIGUE DATA	63
APPENDIX B - REPORT OF INVENTIONS	74

ILLUSTRATIONS

	<u>Page</u>
1. Side Frame Loads	6
2. Truck Bolster Loads	7
3. Average Vertical Side Frame/Roller Bearing Adapter Load Spectrum at 35 mph	10
4. Lateral Wheel Loads on Lead Axle, High Rail with Normal Truck Conditions at 35 mph	12
5. Average Truck Bolster Side Bearing Load Spectrum at 35 mph	13
6. Load Spectra for Side Frame Vertical Load Obtained on 33,000 gallon (100 ton capacity) Tank Car, D-3 Springing	15
7. Load Spectra for Truck Bounce Load Obtained on 33,000 gallon (100 ton capacity) Tank Car, D-3 Springing	16
8. Truck Side Frame Nomenclature	17
9. Truck Bolster Nomenclature	18
10. Estimated S-N Curve for Grade B Steel	23
11. Typical Nominal Design Stresses in Truck Bolster Castings	25
12. Typical Stresses from Vertical Wheel Load	28
13. Typical Stresses from Lateral Wheel Load	29
14. Typical Stresses from 30 bhp Drag Brake Application for 1 Hour	30
15. Expected Fatigue Life of Side Frame and Bolster Castings Using Severe Load Environmental Data	34
16. Expected Life of Side Frame Castings Based on Amplified Levels of Normal Service Load Data	35
17. Thermal and Residual Radial (σ_{rr}) Stresses Across Plate at Hub Fillets, Two-Wear Wheel	39
18. Thermal and Residual Radial (σ_{rr}) Stresses Across Plate at Rim Fillets, Two-Wear Wheel	40
19. Tangential ($\sigma_{\theta\theta}$) Residual Stress Distribution in ksi (MPa) for Cool Rim of Two-Wear Wheel Following 60 Minutes of Tread Brake Application at Indicated Brake Power Levels	44

ILLUSTRATIONS (Concl)

	<u>Page</u>
20. Distribution of Circumferential Rim Stresses Shortly after Brake Application	45
21. Load Application Procedure for Wheel Plate Fatigue Test Fixture	50
22. Wheel Plate Fatigue Test Loading Fixture	52

TABLES

1. Derailments Caused by Truck Component Failures 1965-1974	2
2. Material Properties of Grades B and C Cast Steel	22
3. Material Properties of Wheel Steels	27
4. Crack Growth Rate at Outside Hub-Plate Fillet, da/dn, inches/cycle, from Surface Crack 1/2 inch Long	41
5. Summary of Wheel Plate Fatigue Tests	53

1. INTRODUCTION

1.1 OBJECTIVES

The results of an investigation to evaluate the structural adequacy of freight car truck components and wheels are presented. The primary objective of this work was to assess the structural adequacy of these components with respect to their ability to resist fatigue damage.

Load environmental data which have been obtained on recent test programs and which supplement the data presented in an earlier report of this program (Ref. 1), are also presented. These data provide additional information on the high speed truck bounce phenomenon and its relevance to the accumulation of fatigue damage in freight car truck components.

1.2 BACKGROUND

1.2.1 Reliability Goals - One procedure for evaluating the structural adequacy of freight car truck components would be to compare failure rates with a desired reliability goal. In the absence of such a goal, structural adequacy can be evaluated by determining the conditions which are necessary to cause fatigue damage and the frequency of their occurrence in service.

1.2.2 Failure Rates - Fatigue failures of freight car truck components are relatively rare events when one considers the large numbers of truck components in service. Table 1 lists the number of derailments included in the Federal Railroad Administration (FRA) accident statistics which were caused by the failure of one of the principal freight car truck components. The only defect categories presented in this table are those which would include, but are not necessarily limited to, fatigue or fracture of these components. The data in this table show an increasing trend for accidents due to center plate failures, and a decreasing trend for accidents due to side frame and axle failures. Accidents due to truck bolster and wheel failure are approximately constant for the period covered.

TABLE 1.-DERAILMENTS CAUSED BY TRUCK COMPONENT FAILURES 1965-1974
 (Source FRA Accident Bulletin, Ref. 2;
 FRA Failure Categories Noted in Parentheses)

Year	Bent or Broken			Center Plate (2210)	Wrought and Cast Steel Wheels; Broken Flange, Tread or Rim Defective, Broken Due to Overheating or Other Causes (2305-2312)	Axle Broken Between Journals or Journal Broken Cold (2317 and 2318)
	Freight Car Miles* (10 ⁹)	Side Frame (2201)	Truck Bolster (2207)			
1965	29.3	70	56	22	103	89
1966	30.4	76	41	22	97	99
1967	29.7	63	74	20	107	83
1968	30.1	59	80	26	106	88
1969	30.3	50	81	16	116	106
1970	28.9	40	57	25	83	40
1971	29.2	31	40	26	90	37
1972	30.3	27	57	44	87	40
1973	31.2	37	64	68	112	37
1974	30.7	28	56	65	124	46

* Class I Railroads (Ref. 3)

The number of derailments indicated in this table does not present an accurate representation of the number of components which fail in service. Many components are found to be defective during routine inspections and are removed before they fail. Thus the number of components which become defective under service conditions is substantially larger than the number of component failures which lead to accidents. The AAR Truck Casting Removal Reports, for example, indicate that currently about 1000 truck bolsters and approximately one-fourth this many side frames are removed from service yearly because they are defective.

Although the FRA accident data cannot be used to determine the number of truck component failures per year, they do provide an indication of the relative reliability of these components. For example, if the data from the last 3 years (1972 to 1974) are averaged, the accident rate per component mile (taking into account

the number of components per car) is given as:

Side Frames	- 0.25 accidents per 10^9 side frame miles
Bolsters	- 0.96 accidents per 10^9 bolster miles
Wheels	- 0.44 accidents per 10^9 wheel miles
Axles	- 0.33 accidents per 10^9 axle miles

This tabulation indicates that truck bolsters are the least reliable truck component. Also if center plate accident data were included with the bolster accidents, the rate would be twice that indicated. Because of their relatively low failure rate one can conclude that truck component designs are conservative.

1.2.3 Safety Standards - One of the reasons for reviewing the fatigue strength of freight car truck components is to assess the adequacy of safety standards which apply to these structures. The current FRA railroad freight car safety standards (Ref. 4) call for the periodic inspection of freight car suspension and draft systems. The inspections must take place within 48 month intervals except in the case of high mileage cars where inspections are required every 12 months. The inspection process includes an examination of each of the truck/center plate and coupler/draft gear components to determine if they are functional, if excessive wear has taken place or if there is evidence of the development of cracks. Since most of these structural components are of safe-life rather than fail-safe design it is obvious that the inspection intervals should be established so that there is a minimum probability of failure between inspections. This implies that the rate of crack propagation or of component wear should not allow failure of the parts within the inspection interval. Obviously there is a wide range of operating environments to which cars are exposed in service and the loads tending to develop fatigue or component wear are different with each of these environments. Also the dynamics of each type of car is different so that the internal car and truck forces will vary when cars are exposed to the same type of operating environment.

If the mechanisms of damage were understood through fatigue analysis and test, it would be possible to develop a more rational approach to the establishment of the required inspection intervals. It is known that some components are tolerant to the development of large cracks (e.g., 6 inch) without there being any significant decrease in static fracture strength. With better fatigue data one could determine the period of time (or mileage) required for a crack to propagate from a detectable limit through to a failure condition. A meaningful required inspection period would then be something less than this period of time. Data from flaw propagation studies would therefore make it possible to develop a more rational approach to the establishment of the required inspection intervals. It could lead to different requirements for different classes of equipment and operating conditions.

2. TRUCK COMPONENT LOADS

2.1 LOAD CHARACTERISTICS

Freight car truck components are subjected to a variety of vertical, lateral, and longitudinal loads. In addition, internal forces are developed within the truck itself during the traversal of curved track. Figures 1 and 2 illustrate some of the principal loadings applied to truck side frame and bolster castings. The characteristics of these loads are summarized in the following subsections. More descriptive material may be found in the report from Part I of this program (Ref. 1).

2.1.1 Vertical Loads - The vertical load is the principal load acting on the truck and is due to the weight of the car and lading. The magnitude of this load depends upon the weight of the car and it is modified by transient factors, such as rail irregularities, suspension system oscillations, wheel flat spots, etc. Most of the fluctuations in the vertical load occur at frequencies below 10 Hz. Car rolling motions result in an alternating component of load on each side of the truck at a characteristic frequency of approximately 1 Hz for a loaded car. Car bouncing and pitching motions cause load fluctuations in the 3 to 5 Hz range. The most important influence on the vertical load fluctuations is the characteristics of the spring suspension system, a system having worn control or damping elements resulting in the most severe oscillations and causing large transient loads.

The line-of-action of the vertical load is normally at the center of the bolster, but this can be shifted because of load transfer to one of the side bearings. Load transfer to the side bearings is most severe on curves or during car "rock and roll" motions. Car rock and roll motions are generally the result of a high center of gravity, a truck center distance approaching rail length, operation at critical speed on jointed rail with 1/2 inch or more low joints, and a suspension system not capable of controlling such severe roll input.

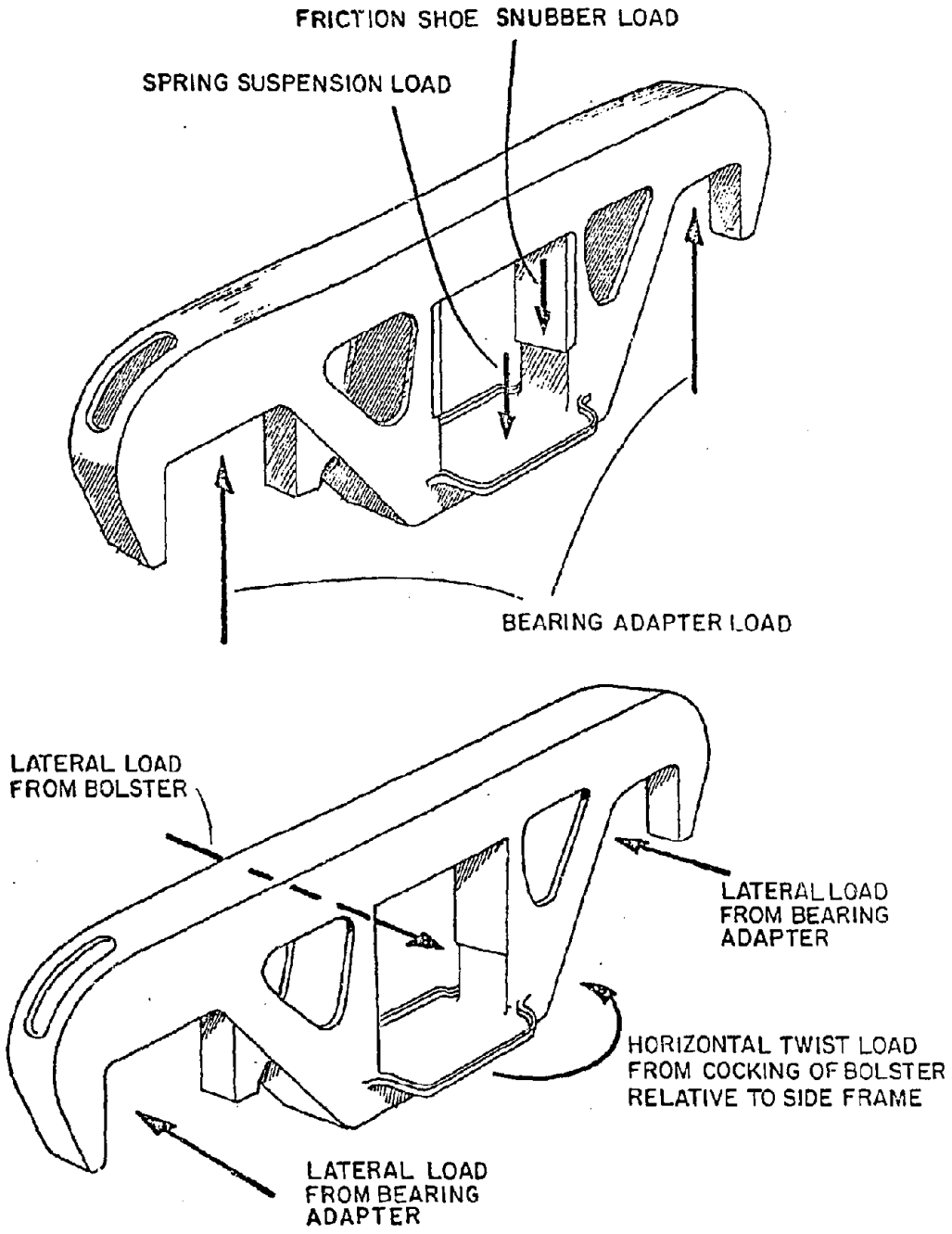


FIGURE 1. SIDE FRAME LOADS

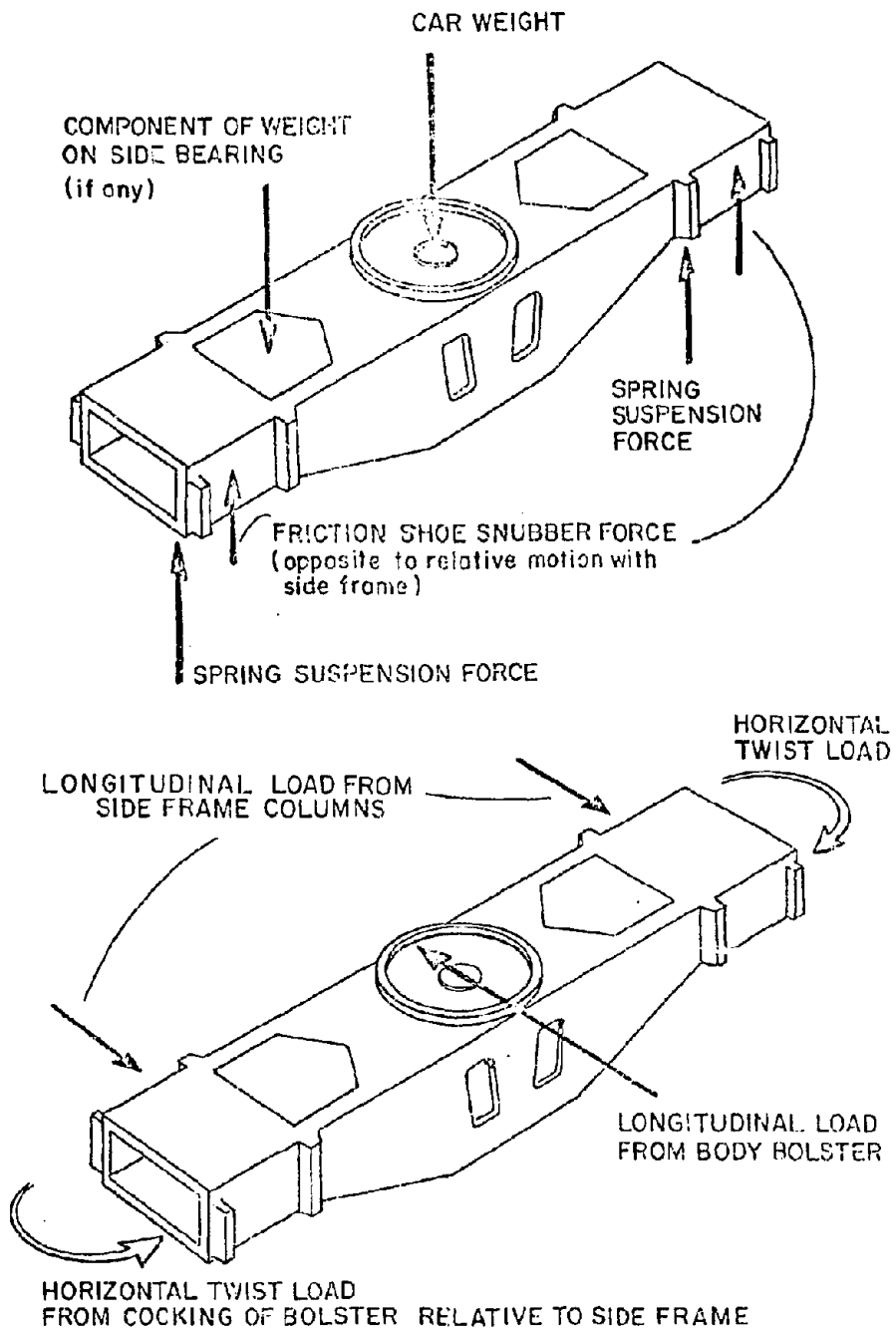


FIGURE 2. TRUCK BOLSTER LOADS

2.1.2 Lateral Loads - Lateral truck loads are the result of load transfer from the car body, such as would be caused by the angularity of the draft force on the car, the superelevation of a curved track rail not commensurate with speed, guiding forces for the negotiation of curves, or flange contacts during the hunting motion of the wheel-axle set. Lateral loads are also associated with the internal truck forces which maintain the truck in a rectangular configuration while traversing curved track. Under these conditions lateral creep and slip forces are built up at the wheel-rail contact points. These forces are normally directed toward the flange. Occasionally large transient forces can be directed in the opposite direction due to guardrail contacts. Severe lateral loads also can be developed at the wheel-rail interface under the self-excited vibrational condition commonly referred to as truck hunting. This condition is usually associated with a lightweight car traveling at high speeds.

2.1.3 Other Mechanical Loads - Horizontal twist between side frame and bolster refers to the moment applied between the end of the bolster and the side frame column in a horizontal plane. It results from the tendency of the side frame to rotate into an out of square position with respect to the bolster during the traversal of curved track or due to truck swiveling motions (truck hunting).

Longitudinal loads result from braking forces and the inertial forces accompanying acceleration of the truck. The most severe forces occur under car impact conditions when an unloaded car is coupled at high speeds into a standing string of cars. The longitudinal load is applied to the bolster at the center plate rim and is reacted at the side frame columns. The load transfer through the center plate rim has been shown to be one of the most severe loading conditions for the truck bolster (Ref. 5).

2.1.4 Wheel Thermal Loads - Wheels are subjected to thermal loading when tread brake shoes are applied. The deposition of this energy in the rim leads to temperature gradients within the wheel. This causes an expansion and twisting of the rim relative to the plate, which induces bending moments and radial tensile

stresses in the plate and circumferential compressive stresses in the rim. The most severe thermal stresses are the high radial tensile stresses developed at the front face hub fillet and the back face rim fillet.

There are two distinct types of severe braking service which lead to large thermal stresses. The first is drag braking which is associated with the descent of a long grade. On some of the long grades in the western mountainous regions this might involve braking for over an hour at moderate rates of energy deposition in the tread of the wheel (e.g., 20 bhp). The relatively long duration of the brake application allows the heat to penetrate through the rim down into the plate. The second type of service is emergency braking. This condition is particularly severe in high speed passenger service where tread brakes are used. Energy deposition rates may exceed 200 bhp for time periods exceeding 2 minutes. The relatively short time of brake application means that most of the heat is retained near the surface of the tread resulting in sharp thermal gradients within the wheel. The high temperatures reached at the tread can also produce metallurgical changes which affect the ability of the material to resist damage.

2.2 MAGNITUDES OF TRUCK COMPONENT LOADS

2.2.1 Summary of Earlier Project Test Data - A series of tests were conducted during this program to measure truck component loads under a variety of conditions. A detailed description of the tests and results was presented in an earlier report (Ref. 1). The principal characteristics of the load environment for moderate speed operations on good track are summarized in Figures 3 to 5. Figure 3 shows a summary of vertical fluctuating loads at the interface between the side frame pedestals and the roller bearing adapters. These data are presented in a load spectrum, which is a plot of the peak levels between mean level crossings (both positive and negative) of the alternating component of the load versus the number of times the load level is exceeded in a given counting interval. Variations in the data are indicated by showing the plus and minus one, standard deviation curves.

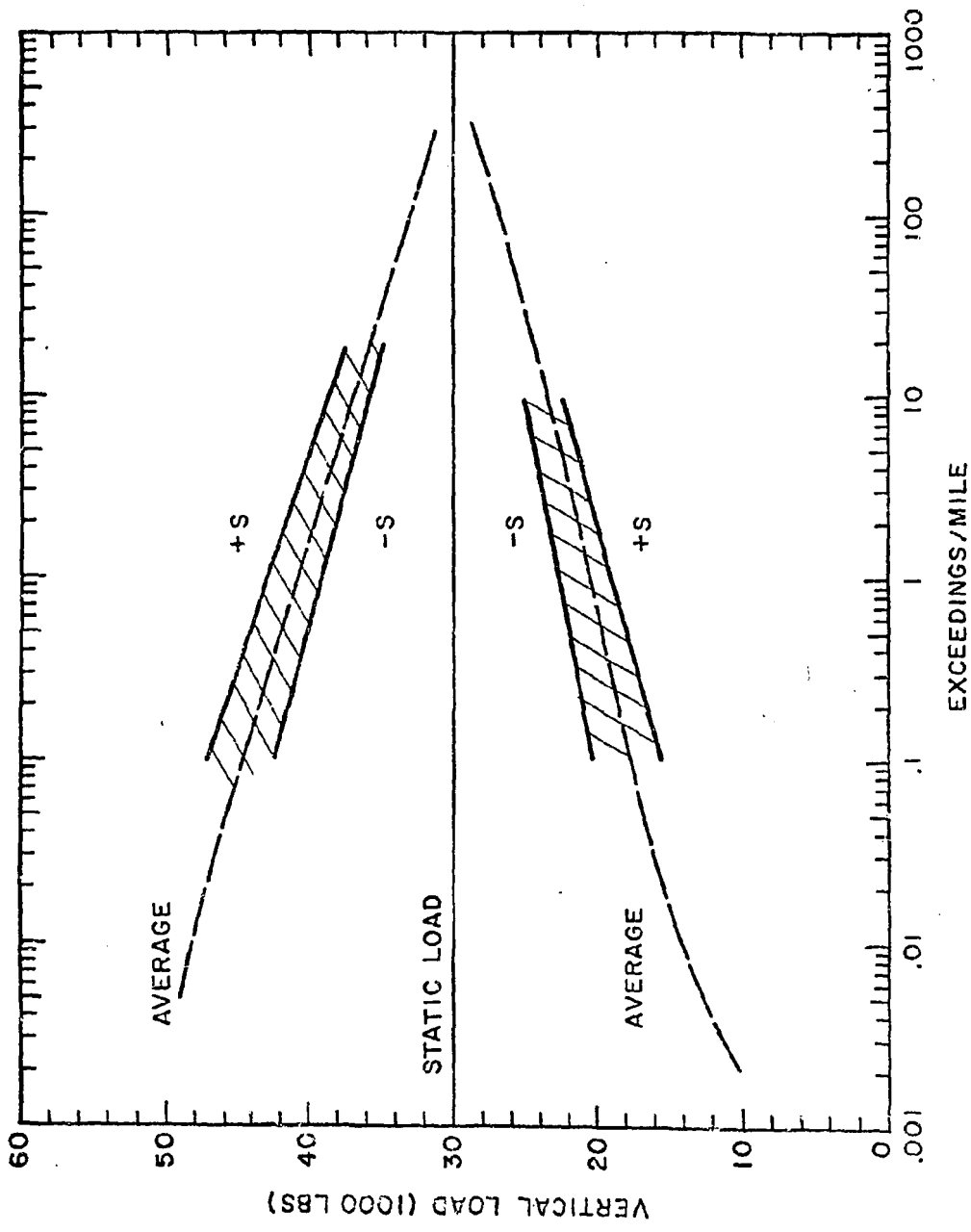


FIGURE 3. AVERAGE VERTICAL SIDE FRAME/ROLLER BEARING ADAPTER LOAD SPECTRUM AT 35 MPH

Figure 4 shows the lateral loads acting toward the flange at the wheel-rail interface. When traversing curved track the highest loads occur on the lead axle at the outside, high rail position. As shown in the figure these loads are a function of degree of curvature. The figure shows both the average peak lateral load and the average load during negotiation of the curve. The spread of the data is indicated by the plus and minus one standard deviation curves. These data are developed for a speed of 35 mph which is slightly above the 30 mph equilibrium speed for the super-elevation of these curves.

Figure 5 shows a load spectra curve for side bearing loads. The intensity of these spectra reflects the roll motions of the car body. The spectra are drawn for the average of the side bearing loads on both sides of the truck. The spread of the data making up the average curve is shown by plotting plus and minus one standard deviation curves.

The data shown in Figures 3 to 5 were obtained on a 100 ton capacity hopper car (6-1/2 by 12 inch journals) operating on good branch line track at 35 mph. The car was loaded to a rail load of 263,000 lbs with iron ore which resulted in a center of gravity of 74 inches above the rail. The car did not develop severe roll motions although it was obvious that the primary excitation of the suspension system was due to a slight to moderate car body roll motions at approximately 1 Hz.

2.2.2 Railway Progress Institute/Association of American Railroads Truck Project Data - Additional truck component load data have become available from various sources. The Railway Progress Institute/Association of American Railroads (RPI/AAR) Truck Research Safety and Test Project has conducted two extensive road tests to gather load data on a 100 ton truck under regular service conditions (Ref. 21). The tests were conducted on eastern and mid-western railroads where most of the movements took place under 45 mph. The instrumented car was loaded with coal and had a relatively high center of gravity of 94 inches. The car had a pronounced tendency to develop roll motions at speeds in the 20 to 25 mph range.

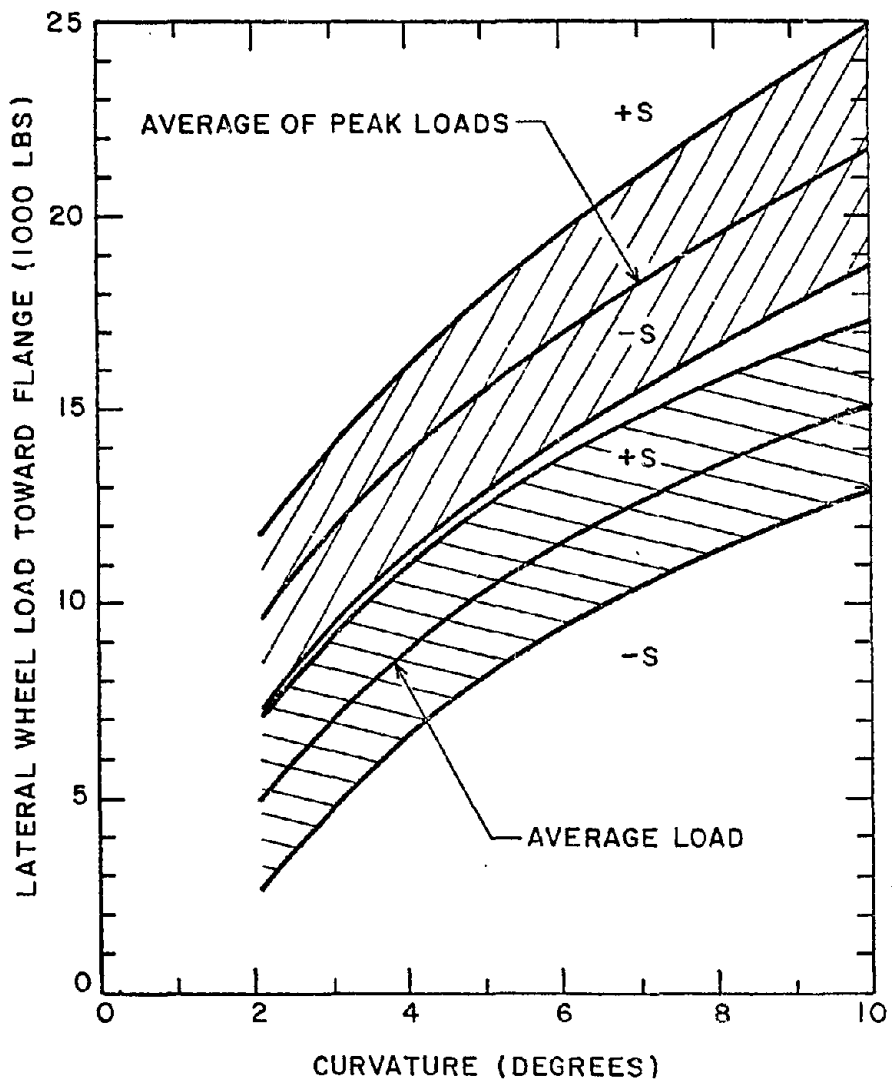


FIGURE 4. LATERAL WHEEL LOADS ON LEAD AXLE, HIGH RAIL WITH NORMAL TRUCK CONDITIONS AT 35 MPH

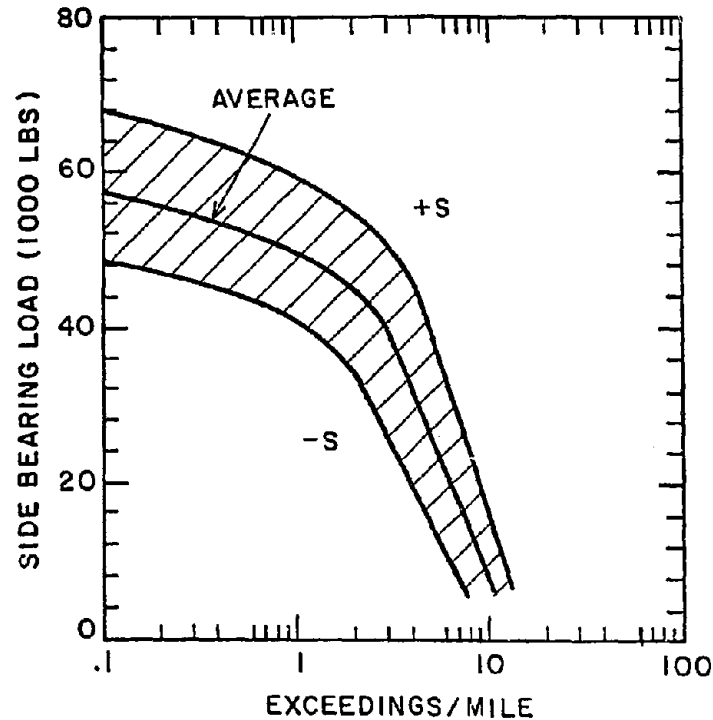


FIGURE 5. AVERAGE TRUCK BOLSTER SIDE BEARING LOAD SPECTRUM AT 35 MPH

The analysis of approximately 1800 miles of data from these road tests indicates that there is an increase of about 30 percent in the intensity of the vertical side frame load spectra from that shown in Figure 3 in a comparable speed range (30 to 45 mph). At lower speeds (15 to 30 mph), where pronounced car body roll motions occur, the increase in intensity of the spectrum is approximately 50 percent. At higher speeds (45 to 60 mph), where truck bounce motions develop, the increase in the intensity of the spectrum is approximately 70 percent.

The RPI/AAR Truck Project data also show a more severe load environment for side bearing loads than that indicated in Figure 5. The increase in the intensity of the spectrum is approximately 20 percent for a comparable speed range (30 to 45 mph) and approximately 15 percent for a higher speed range (45 to 60 mph).

In a lower speed range (15 to 30 mph), where significant car body roll motions occur, the increase in intensity is approximately 70 percent.

The test data from the RPI/AAR project which are available for speeds over 45 mph show the development of significant truck bounce loads. This confirms the limited sample of data presented in Ref. 1. The truck bounce load spectra show a total vertical truck load of 100,000 lbs over the static load once every 50 miles.

2.2.3 Data from Tank Car Tests - Tests were completed in September 1975 on a 33,000 gallon (100 ton capacity) tank car as part of the evaluation of the fatigue characteristics of a prototype tank car head shield. Trucks with instrumented side frames were used to determine the vertical force load environment. The car was loaded with water to the maximum rail load capacity (263,000 lbs). The trucks were equipped with 2-1/2 inch travel springs, which is a somewhat stiffer suspension than the 3-11/16 inch spring travel used in most current freight car trucks. Data from the tests show a severe load environment at speeds above 45 mph. At these speeds severe bounce load oscillations developed and there were many indications of the springs going solid, which resulted in high peak dynamic loads. Figure 6 shows load spectra for the vertical side frame force data from this test run. The data are segregated into three speed ranges, 15 to 30, 30 to 45, and 45 to 60 mph, to show the effect of speed on the intensity of these spectra. Figure 7 shows similar load spectra for the truck bounce load. (This is defined as the instantaneous sum of the two side frame loads.) These data show the effect of the high dynamic loads associated with the suspension springs going solid when operating in the 45 to 60 mph speed range.

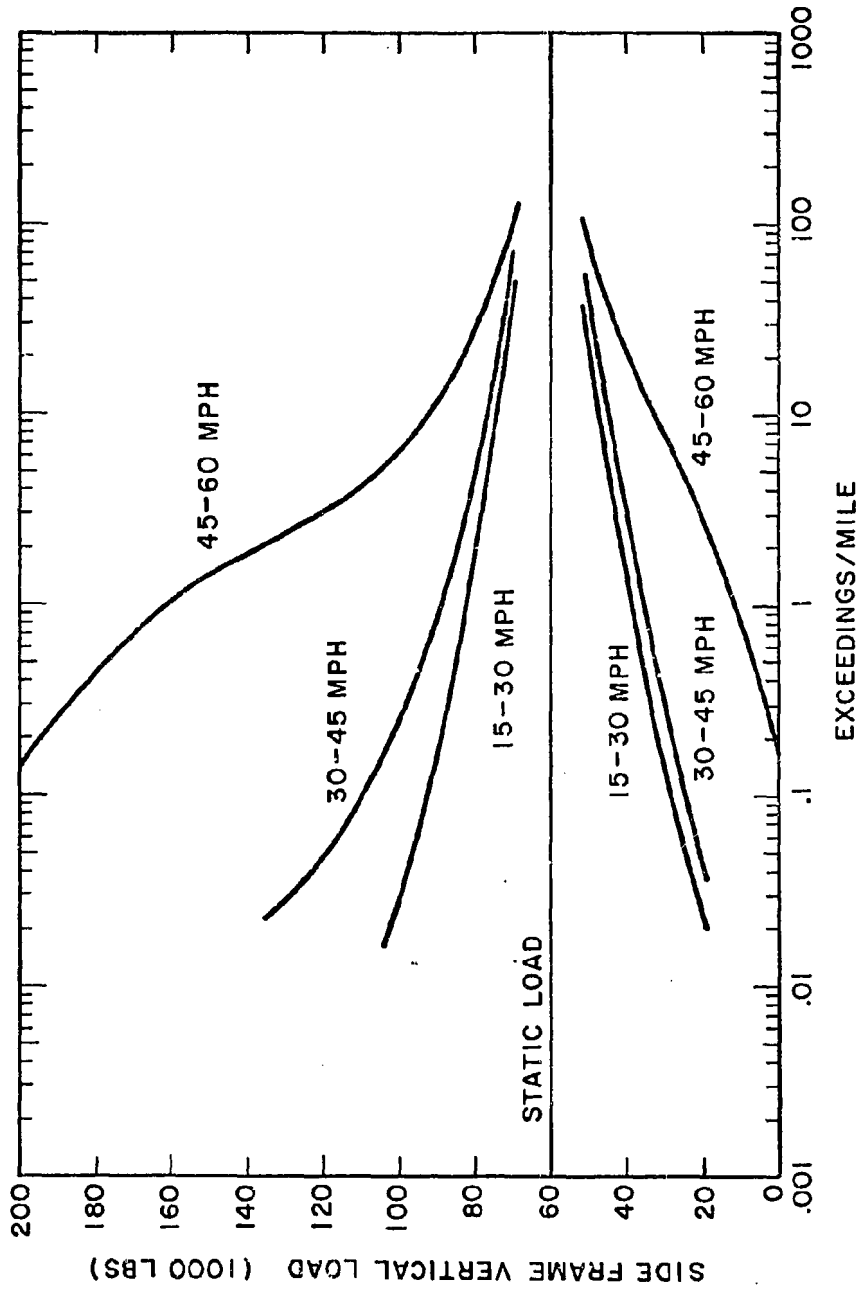


FIGURE 6. LOAD SPECTRA FOR SIDE FRAME VERTICAL LOAD OBTAINED ON 33,000 GALLON (100 TON CAPACITY) TANK CAR, D-3 SPRINGING

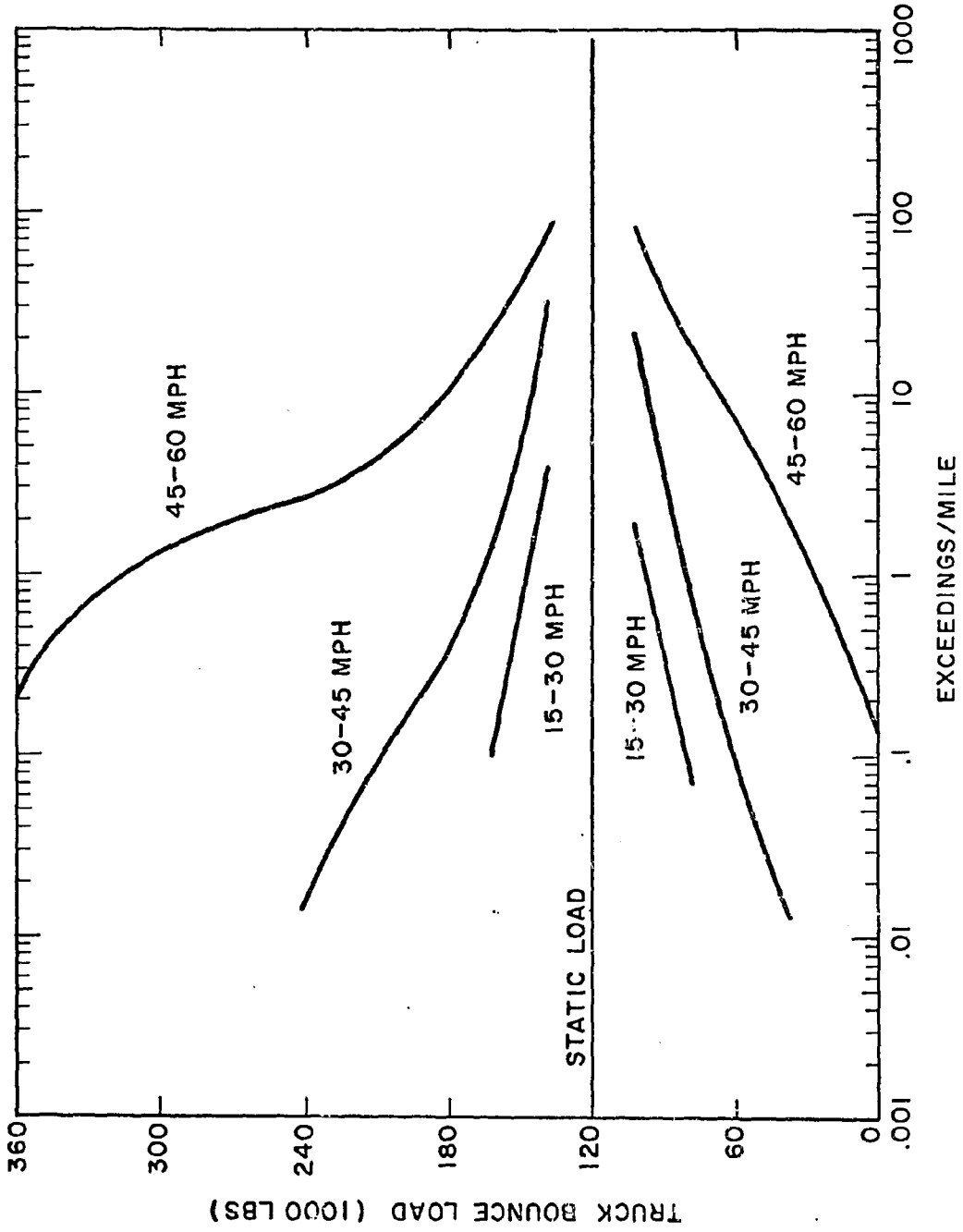


FIGURE 7. LOAD SPECTRA FOR TRUCK BOUNCE LOAD OBTAINED ON 33,000 GALLON (100 TON CAPACITY) TANK CAR, D-3 SPRINGING

3. FAILURE MODES

3.1 TRUCK CASTINGS

Severe wear or evidence of the development of fatigue cracks are the two principal reasons for the removal of truck castings (side frames and bolsters) from service. When severe wear patterns develop they occur at the interconnections between components (e.g., the bolster friction shoe pockets, side frame columns, the bolster center plate area). Because of the complexity of truck casting designs and the inherent characteristics of foundry practice, it is difficult to eliminate all conditions which may lead to the development of fatigue cracks. Fatigue cracks may originate at shrinkage cavities within the castings, the edges of holes, cracking strips, sharp surface corners, or geometrical discontinuities at core joints. These are conditions which cannot be completely eliminated during the manufacture of truck castings.

3.1.1 Side Frames - The most common location for the development of severe wear on a side frame is the column. This type of wear results from interactions with the truck bolster caused by persistent truck swiveling motions or by excessive vertical oscillations resulting from a poorly damped suspension system.

The development of a fatigue crack on a side frame is a relatively rare occurrence. The most common locations are through the tension member (see Figure 8) or through the column. The tension

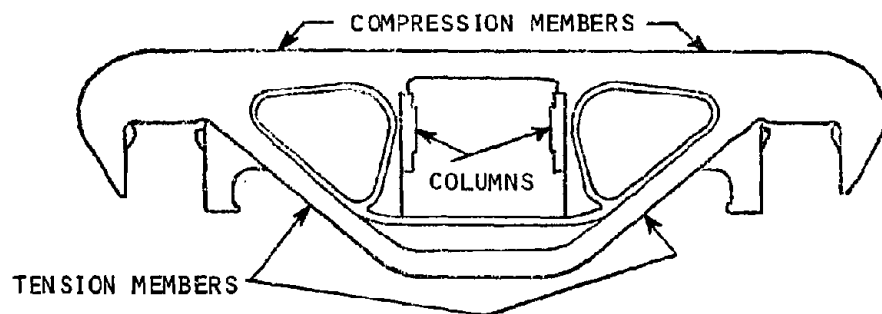


FIGURE 8. TRUCK SIDE FRAME NOMENCLATURE

member crack is the most critical because the propagation of the crack through this member can lead to the collapse of the side frame. On relatively rare occasions fatigue cracks develop in the compression member near the point where it joins the tension member above the pedestal opening.

3.1.2 Bolsters - One of the principal reasons for the removal of bolsters from service is the development of cracked or broken center plate rims. This is generally due to high speed car coupling impacts of empty cars. These conditions result in large truck accelerations and the development of high inertial loads which are transferred to the body center plate through the center plate rim. This leads to severe stresses within the rim (see Ref. 5). Another reason for bolster removal is the development of badly worn center plate rims. The major cause of this condition is uncontrolled truck swiveling motions which occur under high speed operating conditions with lightweight cars.

Bolsters are also removed from service because of the development of fatigue cracks. The most serious location for the initiation of a fatigue crack is on the bottom surface of the bolster because these cracks eventually propagate up the side of the bolster and lead to its collapse. These cracks commonly originate at one of the bottom lightner holes and propagate up to one of the side lightner holes (see Figure 9).

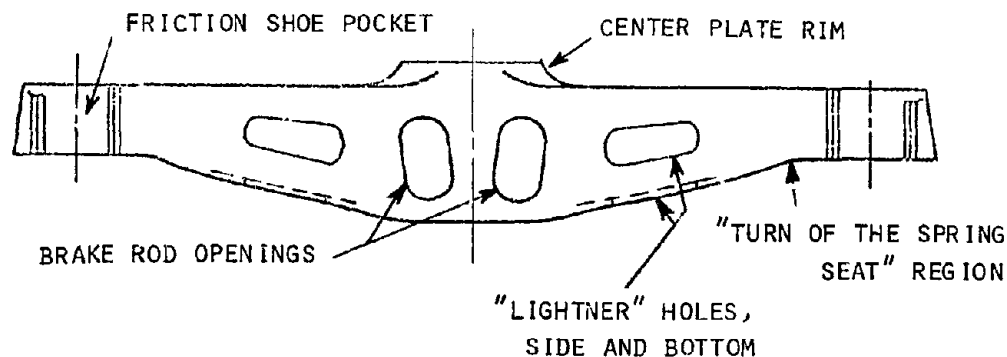


FIGURE 9. TRUCK BOLSTER NOMENCLATURE

Fatigue cracks can also develop at the center of the bolster below the center plate and propagate up through the sides and inside ribs. Cracks on the internal bolster ribs are also a reason for bolster removal. These cracks are often slow growing and their potential for bolster failure is relatively small in comparison with bottom or side surface cracks. Internal rib cracks most often develop under the center plate and with less frequency under the side bearing mounting positions.

The development of fatigue cracks on the bottom surface in the turn-of-the-spring-seat area is a relatively rare occurrence. This, however, is a critical crack location since its continued propagation will result in the collapse of the bolster.

3.2 WHEELS

The AAR Wheel and Axle Manual (Ref. 6) lists 22 types of wheel defects which require removal of wheels from service:

Slid Flat	Overheated
Burnt Rim	High Flange
Shattered Rim	Grooved Tread
Spread Rim	Cracked Hub
Subsurface Defect	Cracked or Broken Flange
Shelled Tread	Cracked or Broken Rim
Out of Round	Thin Rim
Thin Flange	Cracked or Broken Plate
Vertical Flange	Holes Burned in Plate
Thermal Cracks	Loose
Built Up Tread	Out of Gauge

From the standpoint of ensuring the structural adequacy of the wheel the most serious of these defects are thermal (radial rim) cracks, plate cracks and shattered rims.

3.2.1 Radial Rim Cracks - Cracks which originate on the periphery of the wheel and propagate inward toward the hub are commonly referred to as thermal cracks. Once these cracks propagate through the rim they will often turn and propagate as a circumferential plate crack. Sometimes the crack will then reenter and propagate through the rim in a radial direction causing the separation of a large segment of the wheel. A thermal crack might be initiated

and propagate over an extended period of time or the crack may develop rapidly causing a sudden failure of the wheel. Studies of wheels which have failed by thermal cracking have revealed both modes of failure (Ref. 7).

Thermal crack development is associated with modifications in the residual stress field within the wheel which are caused by severe tread braking. Under severe tread braking conditions the periphery of the wheel is heated to a relatively high temperature, but the rim is restrained from expanding by the colder plate and hub of the wheel. This causes the development of circumferential compressive stresses in the rim and radial tensile stresses in the plate. The largest plate stresses occur in the outside hub fillet and the inside rim fillet. If the thermal gradient is large enough, plastic deformation will take place first in the highly stressed plate fillet regions and, with increasing severity of the thermal load, in the rim adjacent to the surface of the tread. If the thermal load causes inelastic deformation in the rim this region will develop residual tensile stress when the wheel cools. The existence of tensile stress in the rim will promote the initiation and growth of thermal cracks.

3.2.2 Plate Cracks - Cracks that initiate in the plate of the wheel and propagate circumferentially around the plate are commonly referred to as plate cracks. They normally develop and propagate as fatigue cracks from a point of initiation in the outside plate hub fillet. Plate crack development is believed to be caused by the effects of both thermal and mechanical loads. The highest stresses in the regions of crack initiation result from the thermal effect, but there are a relatively small number of cycles of high stresses over the life of the wheel. Mechanical wheel loads produce an alternating stress pattern within the critical fillet regions of the wheel once per wheel revolution, but the stress levels are of relatively low magnitude. The relative importance of these stress cycles has not yet been established. An additional factor affecting plate crack growth is that the wheel is more sensitive to fatigue damage from mechanical loads if the

rim of the wheel is heated by tread brake application (Refs. 8 and 9). This results from the steady tensile stresses in the regions where the maximum fluctuating stresses are developed.

3.2.3 Shattered Rim - The development of cracks in the rim slightly below the surface of the tread, and their propagation in a generally circumferential direction so that portions of the tread are broken off, is commonly referred to as spalling or shattered rim failure. It is caused by the fluctuations in the stresses surrounding the wheel/rail contact point as the load is repeated once per wheel revolution. The rolling contact load, if of significant magnitude, will lead to localized yielding in the rim and the development of a residual stress field. The principal component of this stress field is one of circumferential compressive stress. Its maximum value would be slightly below the surface where the shearing stress due to the rolling load is a maximum.

A complete understanding of all factors affecting this mechanism of failure is yet to be developed. It is generally believed that the maximum shearing stress, which lies on a 45 deg plane with respect to the surface, is the critical stress in the development of subsurface cracks. The propagation of these cracks often occurs on surfaces inclined at this angle (Ref. 10). Subsequent redistribution of the stresses causes redirection of the crack toward the surface.

4. DESIGN STRESSES AND THEIR RELATIONSHIP TO FATIGUE DAMAGE

4.1 TRUCK CASTINGS

4.1.1 Material Properties - Side frames and bolsters are cast with steels meeting the requirements of AAR specification M201 (Ref. 11). Almost all castings are made with either Grades B or C steel as defined in the specification. The required properties of these steels are summarized in Table 2.

The anticipated fatigue characteristics of Grade B steel are described by the S-N curve shown in Figure 10. The curve applies to fully reversed stresses of samples with smooth cast surfaces.

TABLE 2.-MATERIAL PROPERTIES OF GRADES B AND C CAST STEEL

Material Property	Grade B *	Grade C #
Minimum yield strength, σ_y (ksi)	38.0	60.0
Minimum ultimate strength, σ_u (ksi)	70.0	90.0
Minimum elongation (percent)	24.0	22.0
Minimum reduction in area (percent)	36.0	45.0

* Grade B castings must be annealed or normalized

Grade C castings must be normalized and tempered or quenched and tempered.

4.1.2 Side Frame Design Stresses - Side frame castings must be designed in accordance with AAR specification M203 (Ref. 12). This specification requires that nominal design stresses[†] must be kept below 16,000 psi in Grade B castings for prescribed combinations of vertical and lateral loads. The corresponding maximum design

[†]The term "nominal" stresses used here refers to the fact that stresses in truck castings are calculated using basic strength of materials concepts, such as the assumption that side frame stresses can be computed as for a simple truss structure or that a bolster can be regarded as a simple beam. No allowance is required in these calculations for stress concentrations due to the presence of holes, lugs, abrupt changes in cross section, etc.

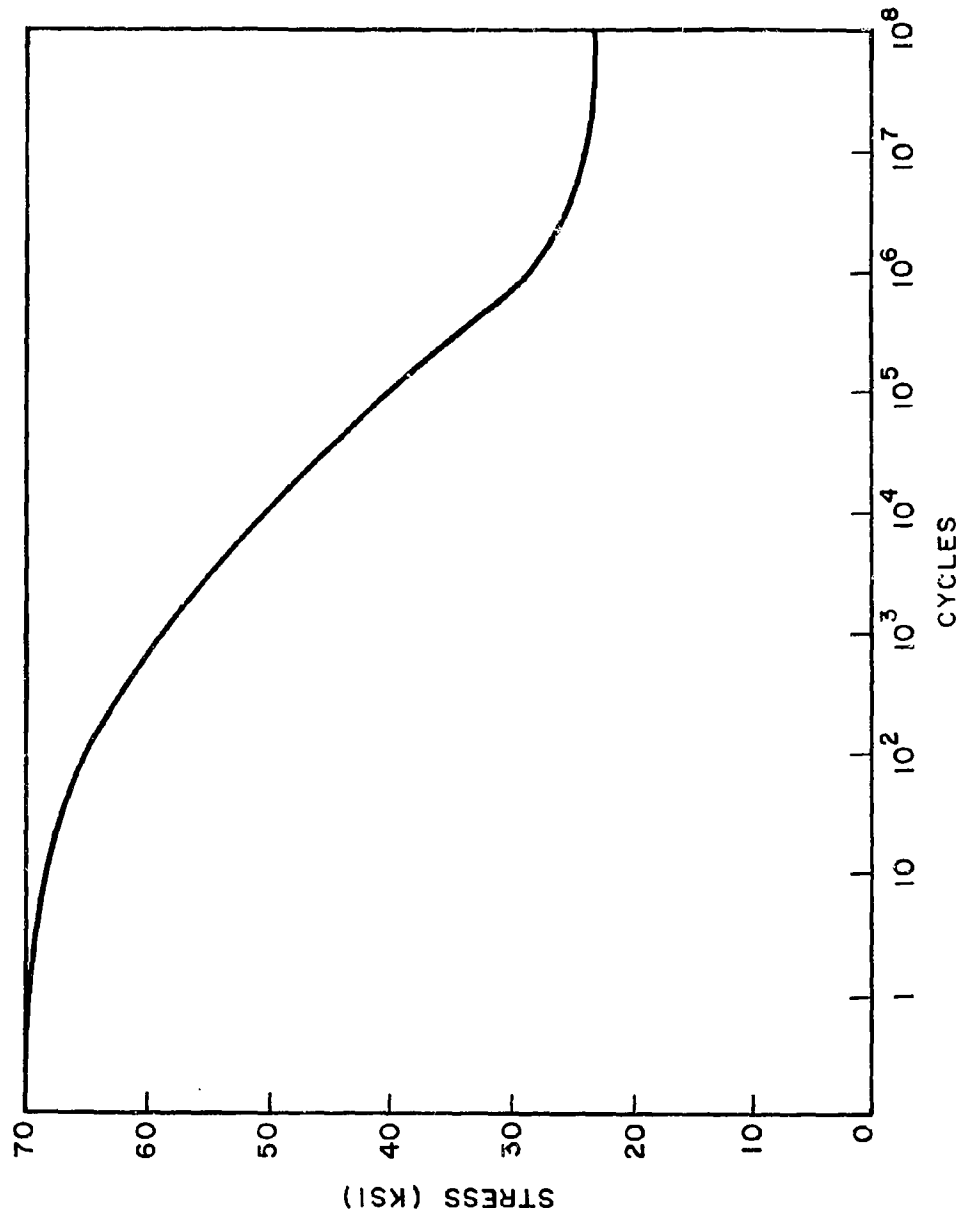
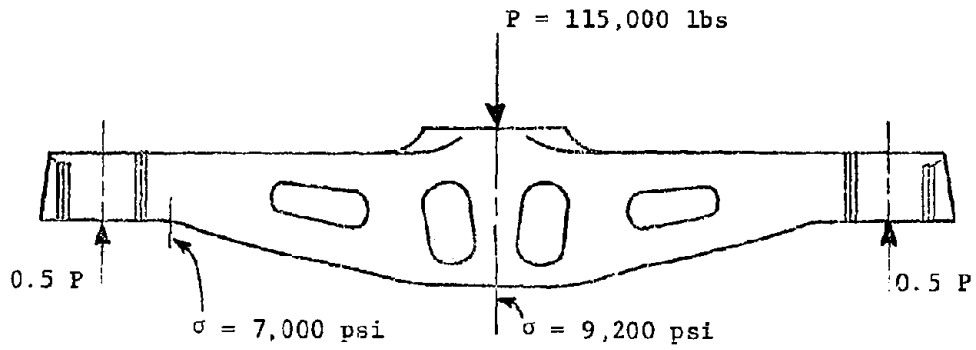


FIGURE 10. ESTIMATED S-N CURVE FOR GRADE B STEEL

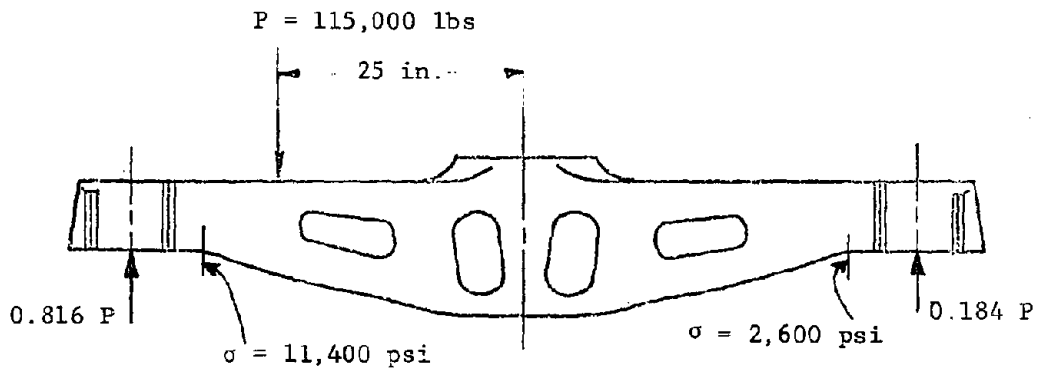
stress for Grade C side frame castings is 25,000 psi. The specified vertical load used in design calculations is 1.5 times the nominal maximum static load on the side frame. For example, the nominal static load capacity for a 100 ton side frame (6-1/2 x 12 inch journals) is a vertical load of 60,000 lbs whereas the design load is 90,000 lbs. The specified horizontal load used in the calculation is given in the specification. In practice, the design stresses are kept somewhat below the maximum allowable stresses. Typically the maximum nominal design stresses due to the vertical static load would be approximately 8000 psi for Grade B steel.

4.1.3 Bolster Design Stresses - Bolster castings must be designed in accordance with AAR specification M202 (Ref. 13). This specification requires that the nominal design stresses must be kept below 16,000 psi in Grade B castings for prescribed combinations of vertical and lateral design loads. The corresponding maximum design stress for Grade C castings is 25,000 psi. The specified vertical design load used in the calculation is the nominal static load. The specified horizontal design load is arbitrarily defined and is related to the vertical design load. The vertical load is the major load influencing the design calculation and must be considered applied at the center of the bolster or over a range of distances from the center. The two major modes of loading which are represented in the design calculation are those due to car body roll where the side bearings are loaded and car body bounce, where load is applied at the center of the bolster.

The vertical design load for a 100 ton capacity truck bolster (6-1/2 x 12 inch journals) is 115,000 lbs, which is approximately the maximum static load. Figure 11 shows typical values of design stresses with Grade B steel at various locations on the bottom of the bolster for both central application of the design load and for application of the load at the side bearing position. For the central application of the load, a typical value for the nominal stress is approximately 9200 psi at the bottom surface at the center.



(A) CENTRAL APPLICATION OF DESIGN LOAD



(B) DESIGN LOAD APPLIED AT SIDE BEARING

FIGURE 11. TYPICAL NOMINAL DESIGN STRESSES
IN TRUCK BOLSTER CASTINGS

At the turn-of-the-spring-seat region the nominal stress on the bottom surface of the bolster is 7000 psi. If the design load is applied at the side bearing position the maximum stress level occurs in the turn-of-the-spring-seat area and is approximately 11,400 psi. At the spring seat region on the opposite side the nominal stress will be approximately 2600 psi.

Note that the weight of a fully loaded car would give higher stresses in the bolster than in the side frame. This results from the fact that the design load for the bolster is the approximate fully loaded car weight on the truck whereas the design load for the side frame is 1.5 times this value. The reason for the difference in design philosophy is the assumption that the side frame will be subjected to higher transient loads than the bolster because the side frame is an unsprung member. The higher nominal stresses in the bolster may be the reason that the failure rate of this component is higher than the failure rate for truck side frames (see Subsection 1.2.2). It should be noted that when the highest loads are developed, such as those reported in Subsection 2.2.3, they occur when the springs are driven solid and thus the suspension system does not provide for alleviation of the load on the truck bolster.

4.2 WHEELS

4.2.1 Material Properties - Railroad wheels are manufactured in accordance with AAR specification M107 (Ref. 14) for wrought steel wheels or M208 (Ref. 15) for cast steel wheels. There are four classes of wheel steels defined in the specifications: U, A, B, and C. The classifications are defined on the basis of carbon content and hardness, as summarized in Table 3. Typical values of yield strength and ultimate strength for these steel classifications are also indicated in the table.

4.2.2 Design Stresses - There are no design stresses specified for wheels. Instead various geometric configurations are specified by stating dimensional requirements (AAR Section G, Ref. 16). Minimum dimensions are specified at critical locations (e.g., plate thicknesses at hub and rim fillets).

TABLE 3.-MATERIAL PROPERTIES OF WHEEL STEELS

Class	Carbon Content (%)	Rim Hardness (bhn)	Typical Values (ksi)	
			Yield Strength	Ultimate Strength
U	0.65 - 0.80		55	110
A	0.57 max	255/321	65 rim 45 plate	105 rim 90 plate
B	0.57 - 0.67	277/341	80 rim 55 plate	135 rim 110 plate
C	0.67 - 0.77	321/363	90 rim 55 plate	140 rim 110 plate

Classes A, B, and C austenitized, rim quenched and tempered.

Typical values for wheel stresses are shown in Figures 12 and 13. The configuration shown is a two-wear 36 inch diameter wrought steel wheel (H 36) which is used on 100 ton capacity cars. Figure 12 shows the radial and tangential stresses at critical, high stress locations, in the plane of loading which result from a 32,000 lb vertical load, the approximate maximum static load for this wheel when installed on a 100 ton capacity car. Figure 13 shows radial and tangential stresses at the same locations for a 10,000 lb lateral load. Note that at critical locations the effect of the lateral load is to counteract the stresses due to vertical load. In both cases note that the magnitudes of the stresses are relatively low. Also note that the variations in stresses from the lower half of the wheel to the upper half are relatively low. This means that as the wheel rotates there are relatively small fluctuating stresses in the body of the wheel. Thus the development of fatigue damage within the wheel from mechanical loading effects would require a discontinuity in the wheel leading to a severe concentration of stresses.

The stresses associated with the heating of the rim of the wheel in a tread brake application are much larger. Figure 14 shows the radial stresses associated with the deposition of 30 bhp on the tread of the wheel for 1 hour. This is a relatively severe case of brake heating, which is representative of the maximum brake heating of wheels allowed in the descent of a long mountain grade.

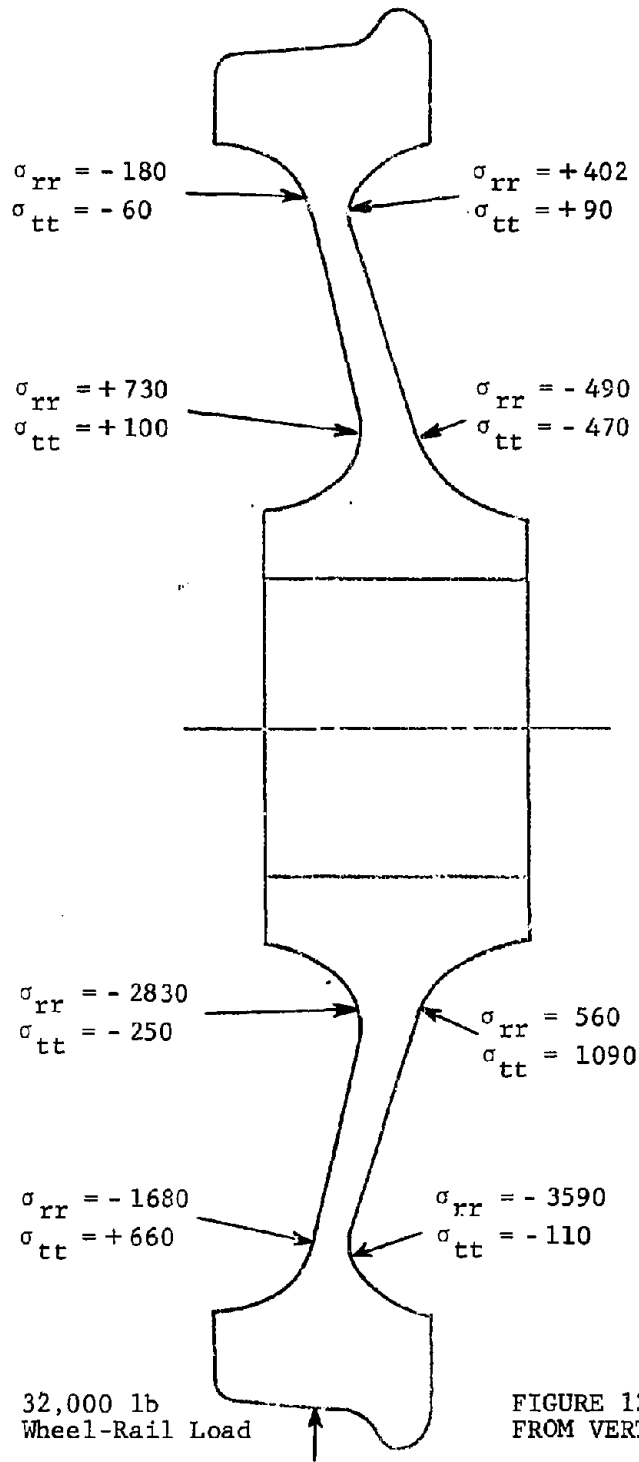


FIGURE 12. TYPICAL STRESSES FROM VERTICAL WHEEL LOAD (lb/in.²)

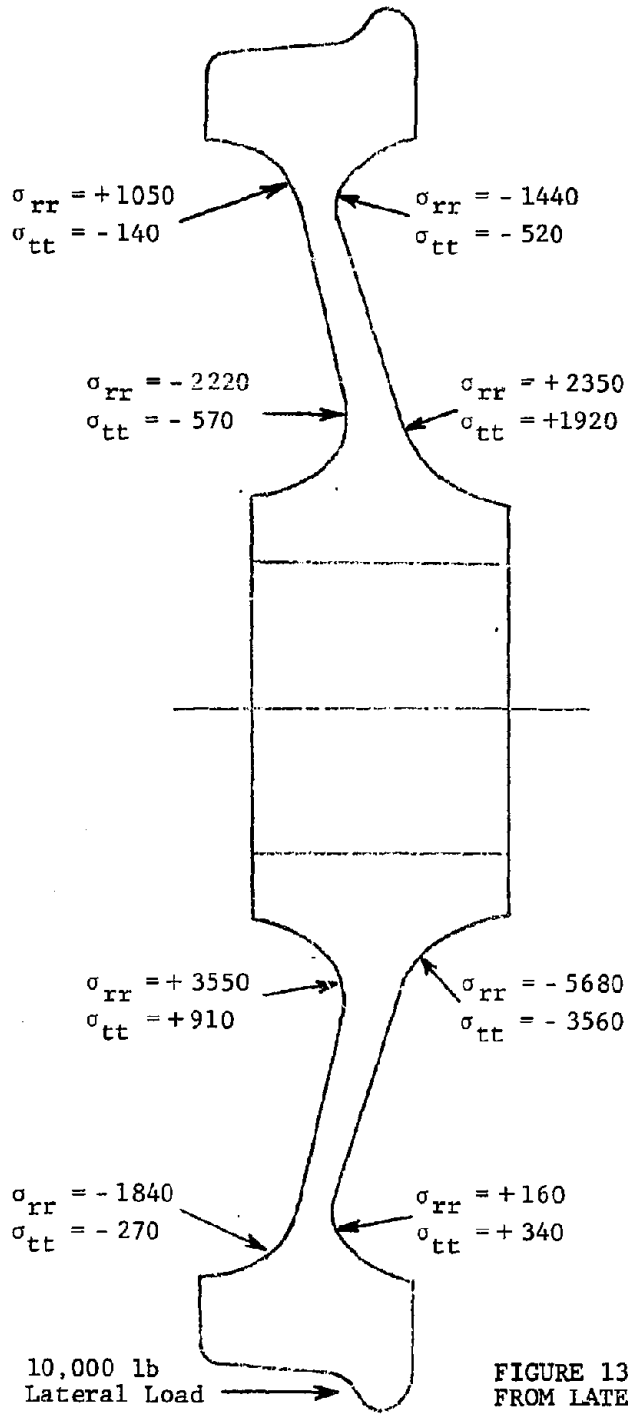


FIGURE 13. TYPICAL STRESSES FROM LATERAL WHEEL LOAD (lb/in.²)

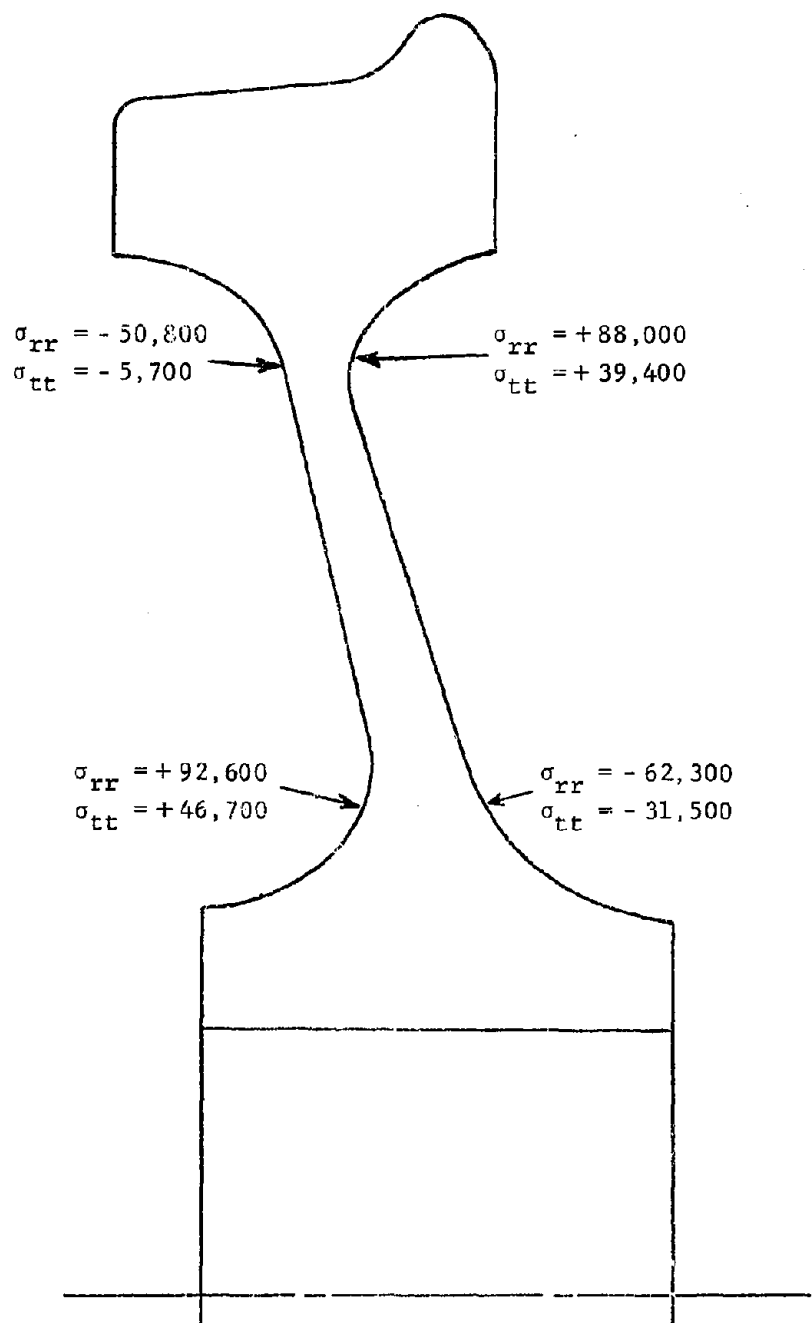


FIGURE 14. TYPICAL STRESSES FROM 30 BHP₂ DRAG BRAKE APPLICATION FOR 1 HOUR (lb/in.²)

Note that the tensile stress in the outside hub fillet and the inside rim fillet are predicted to exceed the yield point of a typical Class U wheel steel. Additional data relating the brake energy deposited in the wheel with thermal stress and the anticipated regions where yielding would take place are presented in Ref. 17.

In addition to the stresses caused by mechanical and thermal loads, the residual stress field within the wheel will affect wheel failures. Some wheels are manufactured in such a way to induce an axisymmetric residual stress field within the wheel. For example, by cooling the rim faster than the plate and hub it is possible to set up a circumferential compressive stress pattern in the rim and a radial tensile stress field in the plate. The circumferential stress in the rim will inhibit thermal crack growth, but the radial tensile stresses in the rim and hub plate fillets will increase the sensitivity for plate crack growth in these regions.

The residual stress field can be modified by several factors. Stresses in the region of the wheel adjacent to the tread are susceptible to modification by the large contact stresses built up in this region. These stresses will be shaken down to a more or less steady state value after a certain period of operations.

The large stresses developed during tread braking (Figure 14) can also modify the residual stress field. Analyses have shown (Ref. 17) that under moderate brake applications the yield point of the wheel will be exceeded in small regions adjacent to the inside rim fillet and outside hub plate fillet. Upon cooling of the wheels there will be a shift toward a compressive radial residual stress in these areas. Residual stress changes in other areas of the wheel will be a minimum. Under more severe tread brake heating yielding can also take place in the circumferential direction in the rim adjacent to the tread. This is due to a combination of the high circumferential compressive stresses which are present in the rim of the hot wheel and the decrease in the

yield strength of the material as the high brake-induced temperatures are reached. When the wheel cools there are resulting regions near the tread where there is a shift in the residual stress field toward a residual tensile circumferential stress.

4.3 FATIGUE EVALUATION

The objective of the fatigue analysis of truck components is to determine the margin of safety between the fatigue strength of these components and the normal load environment they would experience. The objective of the analysis is also to determine the sets of conditions under which this margin disappears and fatigue failures can be expected. Since the fatigue failure rate of truck components is low, one would expect that the development of conditions, whether they be related to component design or train operations, under which failure would be expected is a relatively rare event.

The fatigue evaluations of truck castings which are described in this section are made using the first order fatigue analyses (e.g., linear-damage law, Goodman diagram, and nominal stress levels in the castings). There are a number of difficulties which are encountered when one attempts to apply more sophisticated techniques to the prediction of fatigue damage in these components.

The major problem is in dealing with large stress gradients due to varying casting geometries. There are also problems dealing with stress concentrations in the vicinity of spring lugs, internal ribs, and other such design features. Also, large crack lengths normally develop before failure. This results in large changes in the stress field which affects crack growth. One of the major causes of the development of fatigue cracks is the presence of shrinkage cavities at certain locations. These are regions of high stress concentration. If a crack develops in one of these discontinuities crack propagation often stops outside of the high stress area. An example of this is the spring retention lug on truck bolsters, where under a fatigue test a crack may develop in the base of the lug, but not propagate beyond its width.

4.3.1 Side Frames - Allowable design stresses can be used to perform a first order calculation of the expected fatigue properties of a standard side frame design*. Consider first the maximum fluctuating load data indicated by the RPI/AAR data (Subsection 2.2.2) for the 45 to 60 mph speed range. These data indicate a plus or minus 60,000 lb load superimposed on a 60,000 lb static load would be expected once every 50 miles. Based on a 8000 psi stress for a 60,000 lb vertical load the stress range which occurs with the fluctuating load is zero to 16,000 psi.

One can convert this stress to an equivalent fully reversed alternating stress by using the Goodman diagram assumption. The result is an equivalent alternating stress: $\sigma = +9000$ psi. Referring to Figure 10, this stress is 39 percent of the fatigue limit. In other words, there would have to be a K_f factor of at least 2.5 at the most highly stressed region in the casting for there to be any expected accumulation of fatigue damage.

A different conclusion is reached if one uses the data from the tank car test presented in Subsection 2.2.3. Using the data obtained with the loaded tank car in the 45 to 60 mph range a fatigue analysis is performed similar to the one described above for the RPI/AAR data. These calculations indicate a finite expected fatigue life for K_f factors of greater than 1.4. The results are shown in Figure 15 where the K_f factor is plotted as a function of the expected life for this severe load environment. Note the relatively short life associated with the K_f factor of 3. Since this severe load environment occurred under a unique set of conditions, operating at a critical speed over rough track, one would anticipate that this severe load environment would be associated with only a small percentage of service operations. Note also that small changes in K_f result in large changes in life.

*The details of fatigue calculations presented in this section are included in Appendix A.

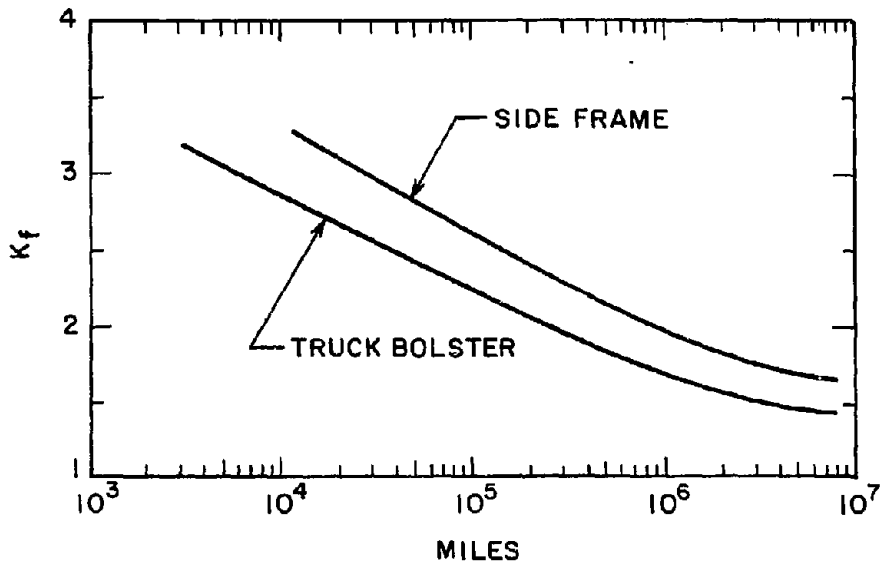


FIGURE 15. EXPECTED FATIGUE LIFE OF SIDE FRAME AND BOLSTER CASTINGS USING SEVERE LOAD ENVIRONMENTAL DATA

The preceding calculations demonstrate that there must be a substantial increase in the normal environmental load or a condition in the side frame casting which leads to a high stress concentration factor or a combination of these two situations for there to be any likelihood of fatigue damage. Additional calculations have been made to illustrate this fact based on the environmental load data presented in Figure 3. Results are shown in Figure 16 where the K_f factor is plotted as a function of expected life for two amplified levels of the load spectra. The amplified environmental load data have been defined as the two and three sigma curves about the average data shown in Figure 3. The curves were developed from calculations using the linear damage law, the assumed S-N curve for Grade B steel illustrated in Figure 10 and an assumed design stress for the static load of 8000 psi.

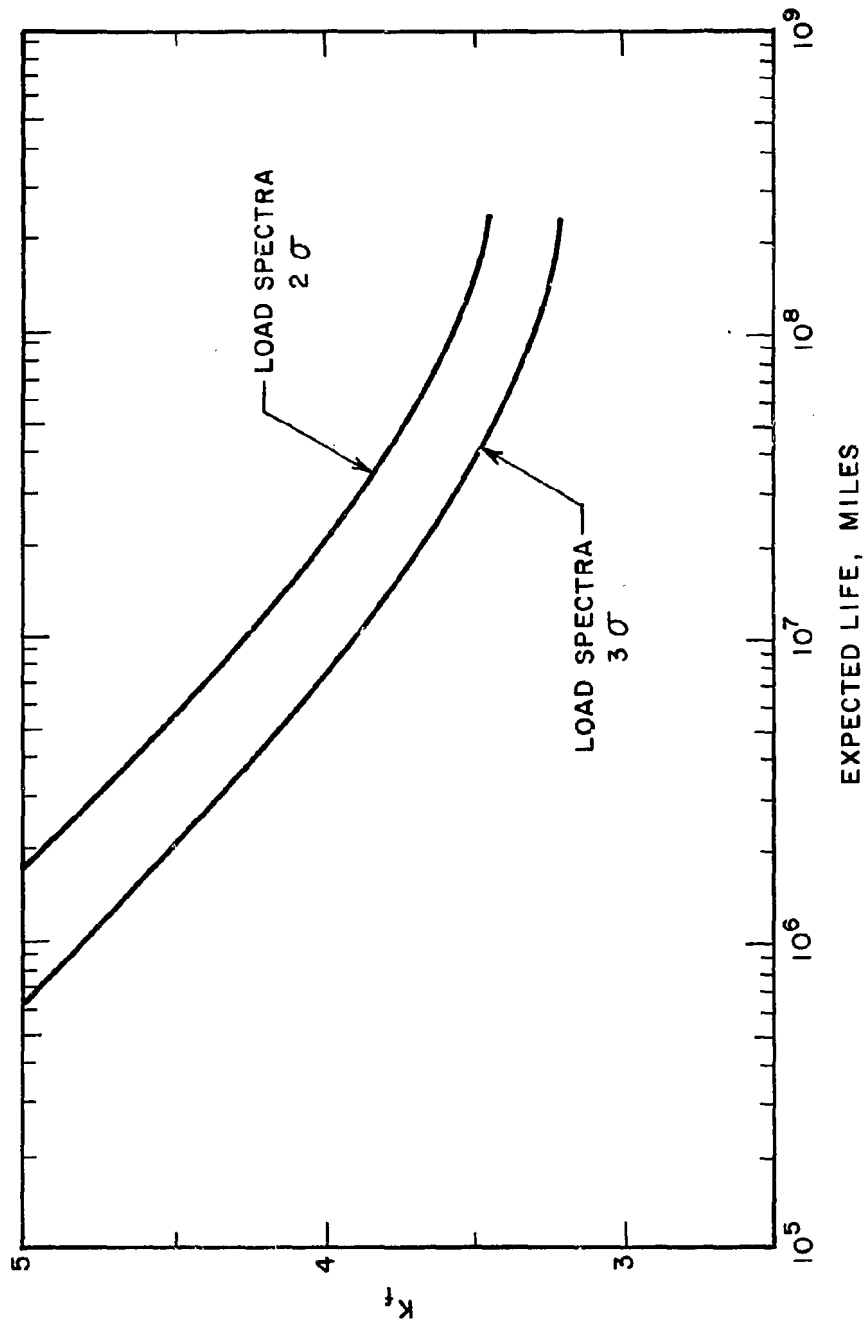


FIGURE 1.6. EXPECTED LIFE OF SIDE FRAME CASTINGS BASED ON AMPLIFIED LEVELS OF NORMAL SERVICE LOAD DATA

4.3.2 Bolsters - Nominal bolster design stresses can be used to perform a first order calculation of the expected fatigue properties of a standard design for the two basic types of loading.

For the bounce load mode of loading consider a load fluctuating from zero to 220,000 lbs. This is a relatively rare event in service. The RPI/AAR data indicate that this might be expected once every 50 miles in the speed range of 45 to 60 mph. Referring to Figure 11 the stress at the bottom of the bolster will vary from zero to 17,600 psi for this load. If one converts this to an equivalent fully reversed alternating stress by using the Goodman diagram assumption this results in an equivalent alternating stress of $\sigma = \pm 10,100$ psi. This is well below the fatigue limit of the material. There would have to be a minimum K_f factor of 2.3 at the bottom of the bolster for fatigue damage to be initiated.

A different conclusion is reached if one uses the data from the tank car tests presented in Subsection 2.2.3. Using the severe bounce load data obtained in the 45 to 60 mph range a fatigue analysis is performed similar to the one described above. This calculation indicates that stress cycles exceeding the fatigue limit would be expected for K_f factors greater than 1.3 and therefore failure would be anticipated in a finite number of miles. The results are shown in Figure 15 where the K_f factor is plotted as a function of the expected life for this severe load data. Since this severe load environment occurred under a unique set of conditions one would anticipate that this environment would be associated with only a small percentage of service operations. Figure 15 also shows that the bolster has a lower anticipated life than the side frame for the same K_f factor. This tends to confirm the data which indicate a higher rate of failure for bolsters than for side frames.

Next consider the effect of alternating side bearing loads on the anticipated fatigue properties of a bolster. Consider the movement of the static load from one side bearing to the other. The RPI/AAR data indicate that this load can be expected once every 100 miles in the speed range of 15 to 30 mph. In the turn of the spring seat region the stress would vary from 2600 to

11,400 psi on the bottom of the bolster. One can use the Goodman diagram assumption to determine that the equivalent fully reversed alternating stress for Grade B steel is: $\sigma = \pm 4900$ psi which is further below the fatigue limit than indicated for the bounce load.

Thus the same conclusion can be reached for the bolster as was reached in the side frame, namely that fatigue failure can be initiated only where there is a severe loading condition or where there is a high stress concentration or some combination of these two conditions.

4.3.3 Wheels - In this discussion two fatigue failure phenomena in wheels, plate crack development, and thermal (radial) crack development, are considered. These are the two most severe fatigue failure phenomena in wheels because they often lead to catastrophic failures resulting in train derailments.

4.3.3.1 Plate Cracks - Previous efforts to analyze the conditions leading to plate crack development have used experimentally measured values of wheel stresses under selected loads to determine the conditions under which plate crack development would be anticipated. Bruner, et al (Ref. 9) determined the stresses in the plate fillet regions for various conditions of vertical, lateral and thermal wheel loads. He also developed S-N fatigue data from sections removed from the wheel. He used the Goodman diagram to convert $R = -1$ fatigue data to stress fluctuations at other mean stress levels.

Carter (Ref. 18) used these stress data and the crack growth properties of wheel steels to compute the minimum crack size under which a crack would propagate for given wheel loads. Both approaches lead to the same general conclusion, namely, that the conditions for crack growth are highly dependent on the presence of quasi-steady radial tensile stresses in plate fillets whether the stresses are caused by a thermal condition or from residual stress effects.

Quasi-steady thermal and residual stresses: let us review the factors which should be considered in the analysis of plate cracks. A primary influence is the presence of a steady or quasi-steady radial tensile stress at the base of the fillet. Relatively

high values for tensile residual stress have been reported in the literature (Ref. 19). Higher residual tensile stresses, exceeding the yield point, can be obtained under prolonged drag brake applications (see Figure 14). However, the percentage of wheel revolutions that would be anticipated under this condition is small.

Analysis indicates that there will be a shift in the residual stress field in the plate following a severe drag brake heating. Consider the thermal stresses illustrated in Figure 14. Figures 17 and 18 show the distribution of radial stresses across the plate for the thermal stress associated with a hot wheel and the change (from a zero value) of residual stresses following cooling of the wheel. Note that where high thermal tensile stresses are developed, at the inside rim and outside hub fillets, radial compressive residual stresses result. This would tend to inhibit plate crack growth. Note also the sharp stress gradient through the plate shown by these figures. If a crack is initiated at the surface it will encounter different stress levels as it grows into the plate. The presence of the crack will also affect the stress field and this effect will not necessarily be detrimental. The presence of a crack could, for example, increase the local flexibility of the plate resulting in a lowering of stresses.

Fluctuating stresses caused by mechanical loads: the second factor to be considered is the effect of fluctuating stresses due to mechanical loads (lateral and vertical) coupled with the rotation of the wheel. The fluctuating stresses from these effects were illustrated in Figures 12 and 13. These stresses are below the level which would lead to fatigue damage. Even if one were to double the vertical load, which could represent the dynamic load effects due to suspension system oscillations, or consider a 10,000 lb lateral load acting against the flange, the fluctuating stresses are below the threshold of fatigue damage. Also, both these effects tending to increase load would be expected only during a very small percentage of the lifetime of the wheel. Only when these stresses are combined with high values of residual tensile stresses will they be of possible significance in the development of fatigue damage.

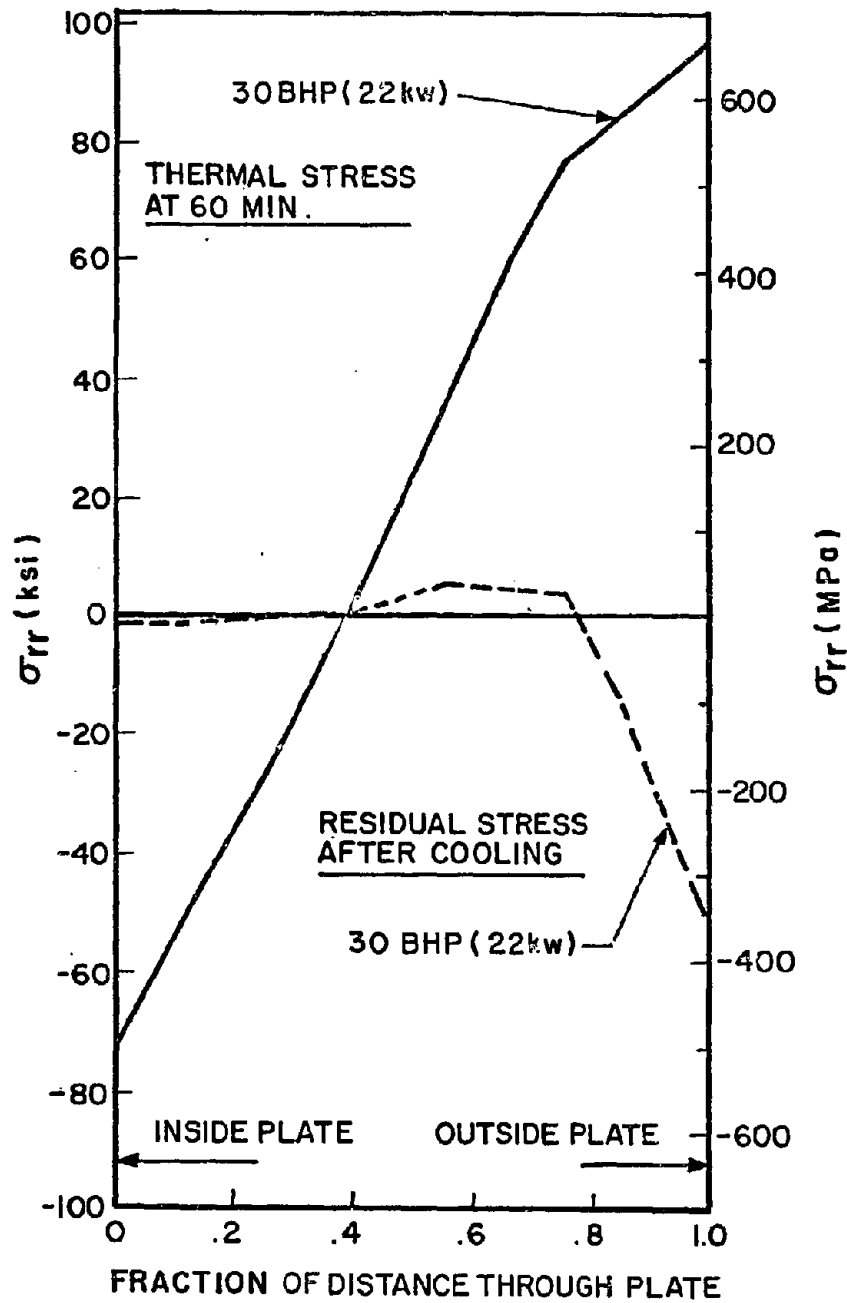


FIGURE 17. THERMAL AND RESIDUAL RADIAL (σ_{rr}) STRESSES ACROSS PLATE AT HUB FILLETS, TWO-WEAR WHEEL

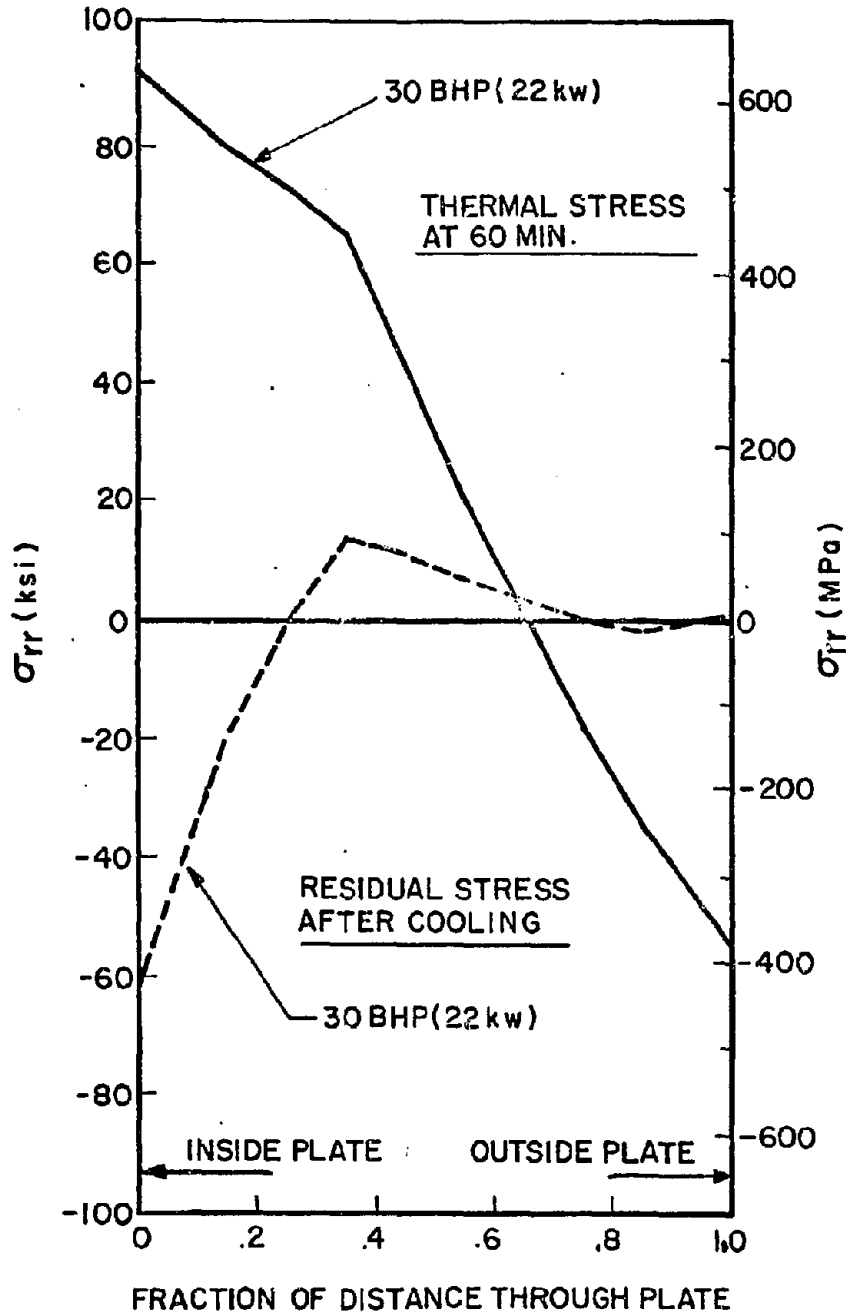


FIGURE 18. THERMAL AND RESIDUAL RADIAL (σ_{rr}) STRESSES ACROSS PLATE AT RIM FILLETS, TWO-WEAR WHEEL

Service brake applications: a third factor to be considered is the effect of moderate thermal strains which are developed under service brake applications. These brake applications occur more often during the lifetime of the wheel than sustained drag brake applications. In fact, many wheels may never experience the sustained drag brake application associated with the descent of a long mountain grade. A moderate brake application (e.g., 20 bhp for 5 minutes) can cause radial thermal tensile stresses at the inside rim and outside hub plate fillet regions on the order of 15,000 psi. These stresses can be significant for plate crack growth, particularly if they are associated with moderate levels of residual tensile stresses.

The preceding information can be summarized by reviewing results from a series of calculations relating crack growth from a plate flaw through various combinations of loads. The results of the calculations are shown in Table 4. These calculations are based on the assumption of a plate crack 1/2 inch long and crack growth properties given in Ref. 18. The fracture toughness of the material is assumed to be 35 ksi (inch)^{1/2}. The minimum change in stress intensity which causes crack propagation is assumed to be 6 ksi (inch)^{1/2}. The effect of mean stress is taken into account by the Forman relationship. The decrease in stress as the crack propagates into the plate is neglected in this calculation.

TABLE 4.-CRACK GROWTH RATE AT OUTSIDE HUB-PLATE FILLET, da/dn, INCHES/CYCLE, FROM SURFACE CRACK 1/2 INCH LONG

Wheel Load Condition	Quasi-Steady Radial Stress (psi)						
	-10,000	0	10,000	20,000	30,000	40,000	50,000
Static Vertical Load	nil	nil	nil	nil	nil	nil	nil
Twice Static Vertical Load	nil	nil	9.2×10^{-8}	2.7×10^{-7}	9.0×10^{-7}	∞	-
Static Vertical Load with 20,000 lb Lateral Load	nil	nil	1.6×10^{-7}	4.5×10^{-7}	1.9×10^{-6}	∞	-
Static Vertical Load with Service Brake Application*	nil	7.1×10^{-7}	2.8×10^{-6}	1.5×10^{-5}	∞	-	-

* Maximum brake application stress assumed +15,000 psi. Calculation here refers to crack growth with one cycle per brake application.

The results presented in the table show that the value of the quasi-steady radial stress in the plate of the wheel is the major parameter affecting crack growth. Results in the first row show that the static vertical load will not produce fatigue damage regardless of the magnitude of the residual stress because the change in stress intensity is below the threshold for crack growth. Data in the second row, where a dynamic enhancement of the static stress by a factor of 2 is assumed, show that the crack can propagate if the steady stress is high enough, but this is a very low probability combination of loads. The third row shows a similar conclusion. Severe lateral loads coupled with steady radial stresses can cause fatigue damage, but again this is a very low probability event. The fourth row shows that the service stresses associated with normal brake applications can produce a growing crack and the rate of crack propagation increases with increasing residual tensile stresses. Note, however, the frequency of this load application would be quite low. Nevertheless there does appear to be a radial stress threshold about 20,000 psi where crack growth could be initiated at a fairly rapid rate from this particular combination of stresses.

The preceding work shows that it is necessary to get answers to the following questions before meaningful fatigue analysis can be made to describe the growth of plate cracks.

- a) Will residual radial compressive stress develop at the surface of the inside rim fillet and the outside hub fillet following a prolonged drag brake application of moderately high brake energy input?
- b) If such a compressive layer is developed does it prevent crack growth in this region?
- c) What is the relative effect on crack extension of the following phenomena: fluctuating stresses due to vertical load with wheel rotation under high thermal stresses, fluctuating stresses due to vertical and lateral loads with wheel rotation under various residual stresses, fluctuating stresses due to brake applications?
- d) What is the effect on crack extension caused by the sharp stress gradients through the plate?

One must recognize that in many cases cracks of considerable length may develop in wheels before there is a catastrophic failure of the wheel. Cracks may also alleviate stresses reducing the crack growth rate. At a minimum they will result in modifications of the stress field.

4.3.3.2 Thermal Cracks - The analysis of the growth of thermal cracks is difficult because of the limited quantitative data available. The phenomenon is generally believed to be related to modifications of the residual stress field following severe brake heating. The critical modification is one which causes the development of residual circumferential tensile stresses near the tread when the wheel cools. A surface defect in the wheel or material damage caused by a local hot spot is then sufficient to initiate the development of a crack. Its initial propagation into the rim would probably be influenced by the once per revolution contact stress variations. More analytical work is required to determine the properties of contact stress phenomena as it affects the initial stages in the growth of radial thermal cracks.

Analysis of the response of wheels to severe drag brake applications (Ref.17) has indicated how residual circumferential tensile stresses can develop adjacent to the tread of the wheel. Figure 19 shows the residual compressive stresses in the rim of a two-wear wheel after the wheel has cooled to ambient temperature following the application of 30 and 40 bhp. Both wheels experience large compressive stresses in the rim while hot. Residual stresses in the 30 bhp wheel are negligible, but in the 40 bhp wheel there is a thin layer of steel adjacent to the tread where the residual tensile stress exceeds 20 ksi. This position of the wheel was heated to approximately 900°F during the brake application, which lowered the yield point allowing the material in this region to be deformed plastically.

Once a thermal crack has been initiated other mechanisms may serve to drive the crack deeper into the rim. One of these is illustrated in Figure 20. The effect occurs during the first

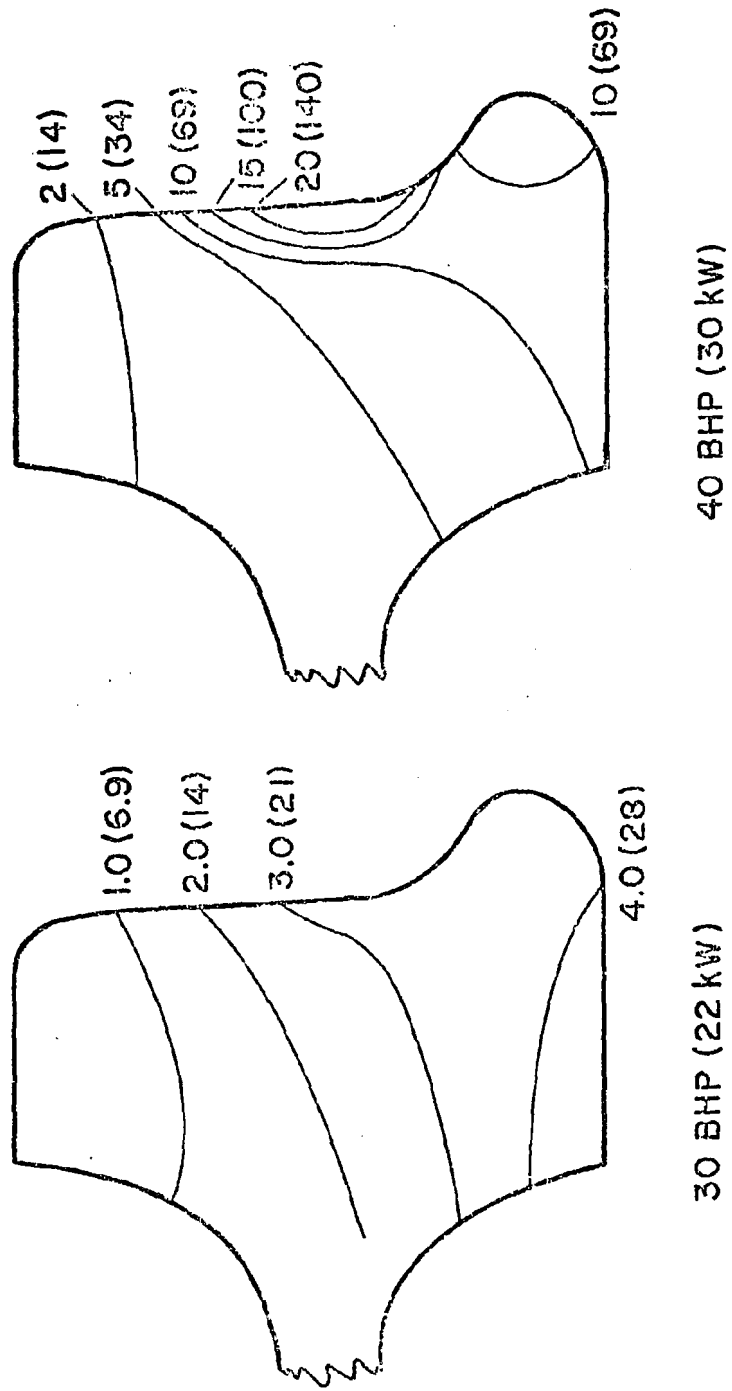


FIGURE 19. TANGENTIAL (σ_{tt}) RESIDUAL STRESS DISTRIBUTION IN KSI (MPa) FOR COOL RIM OF TWO-WEAR WHEEL FOLLOWING 60 MINUTES OF TREAD BRAKE APPLICATION AT INDICATED BRAKE POWER LEVELS

minute or two of a tread brake application. The surface layer of material at the tread is heated by the deposition of the brake energy, but there is insufficient time for the heat to be conducted all the way down into the rim. Therefore, the thermal gradient is quite steep resulting in circumferential compressive stresses in the outer layer of the rim and tensile stresses in the cold metal below. The tensile stresses could cause the inward propagation of a thermal crack. The existence of this phenomenon has been noted on data obtained from wheel-mounted strain gages during brake tests. However, stress calculations have not yet been performed to obtain the quantitative stress data which are necessary to evaluate its significance as a driving mechanism for thermal cracks.

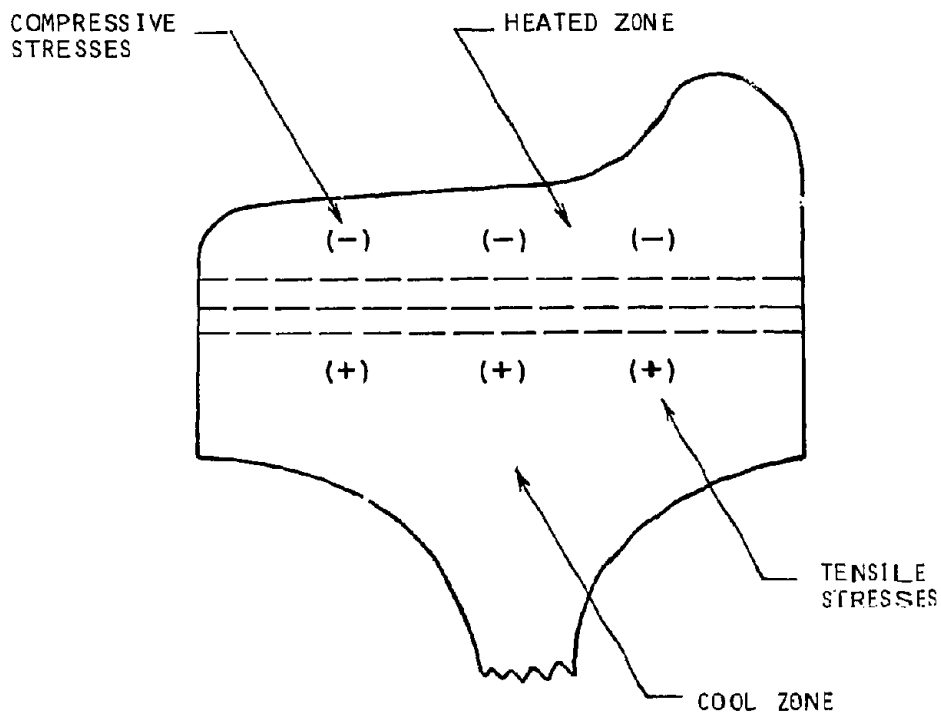


FIGURE 20. DISTRIBUTION OF CIRCUMFERENTIAL RIM STRESSES SHORTLY AFTER BRAKE APPLICATION

The once-per-wheel-revolution repetition of high stresses in the vicinity of the contact zone is another possible mechanism for driving a thermal crack into the rim. Cold working of the tread may result from these stresses producing effects related to radial crack growth.

In summary, it is impossible to determine analytically the safety margin of wheels with respect to the development and propagation of thermal cracks. More data are required on the magnitude and duration of thermal brake loads which lead to the development of residual circumferential tensile stresses in the rim. In addition, the effects of stress fluctuations caused by contact stresses, and the role of short term brake application thermal stresses in the propagation of these cracks must be determined.

5. FATIGUE TEST DATA

The evaluation of structural adequacy of freight car truck components with respect to fatigue could best be accomplished by conducting fatigue tests where the fluctuating loads were representative of the loads experienced in service. There is a limited amount of such fatigue test data available.

5.1 SIDE FRAMES

Side frame data can be obtained from the fatigue test requirement for side frames which is part of AAR specification M203 (Ref. 12). This specification calls for new side frame designs to be tested in either the ASF or Dresser side frame fatigue test machines. The machines apply a complex pattern of vertical, lateral, twist, and impact loads on side frame castings. The requirement calls for testing of a group of four sample castings which must undergo an average of 100,000 cycles of load without the development and extension of a transverse crack to 1/2 inch. The minimum number of cycles for any one of the four sample castings is 50,000 cycles.

This requirement can be used to determine an upper limit for the K_f factor for side frames. Only the vertical load component for a 100 ton capacity truck side frame is considered in this example. For this type of casting the ASF fatigue machine utilizes a vertical loading cycle from zero to 150,000 lbs.* Using the data previously presented for Grade B castings, a stress range from zero to 20,000 psi would be expected based upon an 8000 psi stress at a design load of 60,000 lbs. If one then converts the stress range to the equivalent fully reversed alternating stress using a Goodman diagram the result is $\sigma = \pm 11,700$ psi.

Figure 10 indicates that the expected fatigue stress at 100,000 cycles for Grade B steel is $\sigma = \pm 39,500$ psi. Therefore an upper limit of K_f for an average side frame is

$$K_f < \frac{39.5}{11.7} = 3.4$$

* The Dresser machine varies the vertical load from 50,000 to 150,000 lbs and in addition includes the impact load effects of a falling weight while under maximum load.

In all probability the actual K_f factor is less than this because the average side frame has a fatigue life substantially greater than the 100,000 cycles that must be demonstrated in the specification test.

5.2 WHEEL FATIGUE TESTS

5.2.1 Background - As part of this program fatigue tests were conducted on wheels in an attempt to obtain data which would lead to a better understanding of the development of plate cracks. These tests were also planned to evaluate techniques for performing fatigue tests on wheels. A complete simulation of service stresses on wheels would require a complex loading fixture capable of subjecting rotating wheels to the thermal load from a tread brake, and vertical and lateral loads representative of forces at the wheel-rail interface. The development of such a fixture was beyond the scope of the program. Instead, it was believed that the structural adequacy of wheels with respect to plate crack initiation and development could be studied by utilizing a loading fixture which applied alternating lateral loads to the wheel. Lateral loading of the wheels was selected to study this effect because it leads to larger plate stresses than vertical wheel loading (Figs. 12 and 13).

The results of two previous experimental investigations of wheel plate fatigue are important to consider when planning new plate fatigue tests. Wetenkamp, et al (Ref. 20) attempted to determine the fluctuating stresses which would cause wheel plate fatigue by subjecting a rotating wheel-axle set to lateral loads applied against the rim. A fixture was constructed which allowed the application of lateral loads through spring loaded rollers on the outside surface of the rim on each wheel. Class C wrought steel 36 inch diameter, wheels of "thin plate" and "thick plate" design were tested in this fixture. The wheels were subjected to 17,000,000 stress cycles (equivalent to 30,000 miles of operation) with a 20,000 lb lateral load acting against the rim. No cracks developed during this test period. The stress range produced by rotation with the 20,000 lb lateral load imposed was approximately four times the magnitude of the stress range produced by a representative service loading of 20,000 lbs acting vertically and 8000 lbs acting laterally.

Bruner, et al (Ref. 9) loaded a B33 wrought steel wheel vertically and laterally at the tread and measured the resulting stresses in the plate. They also heated the rim to simulate tread brake heating effects and measured the resulting thermal strains. The results were used to develop typical patterns of fluctuating stresses which were representative of service load conditions in order to determine the possibility of producing fatigue damage in the wheel plate. A number of 2 inch wide radial sections were cut from these wheels and subjected to alternating loads to determine the fatigue strength of the plate. Sufficient data were obtained to develop an S-N curve for the wheel plate material. A fatigue limit of 22,500 psi for fully reversed stresses was indicated. Comparing service stresses with the fatigue strength data indicated that a combined condition of severe rim heating (70 minutes drag brake) and severe lateral loads (20,000 lbs) were required for the development of fatigue damage to be expected.

The objective of the fatigue tests which were conducted under this program was to determine the margin between fatigue strength of the wheel plate and the fluctuating plate stresses which occur because of vertical and lateral loads. It was anticipated that lateral loads of approximately 50,000 lbs would be required to develop plate cracks. The development of a loading fixture applying lateral loads to a rotating wheel such as used by Wetenkamp would be difficult under these circumstances. Therefore it was decided to develop a fixture where alternating lateral loads would be applied at diametrically opposite positions to the rims of two wheels which were mounted on an axle. This permitted a simulation of alternating wheel plate stresses which are caused by lateral loads acting toward the flange of the wheel as it rotates. The simulation of alternating stresses would occur at two diametrically opposite positions on the wheel.

The principle of operation of the test fixture is illustrated in Figure 21. Lateral loads are applied through a loading frame against the side of the rim at diametrically opposite positions on the wheel. The loads are developed by two hydraulic cylinders

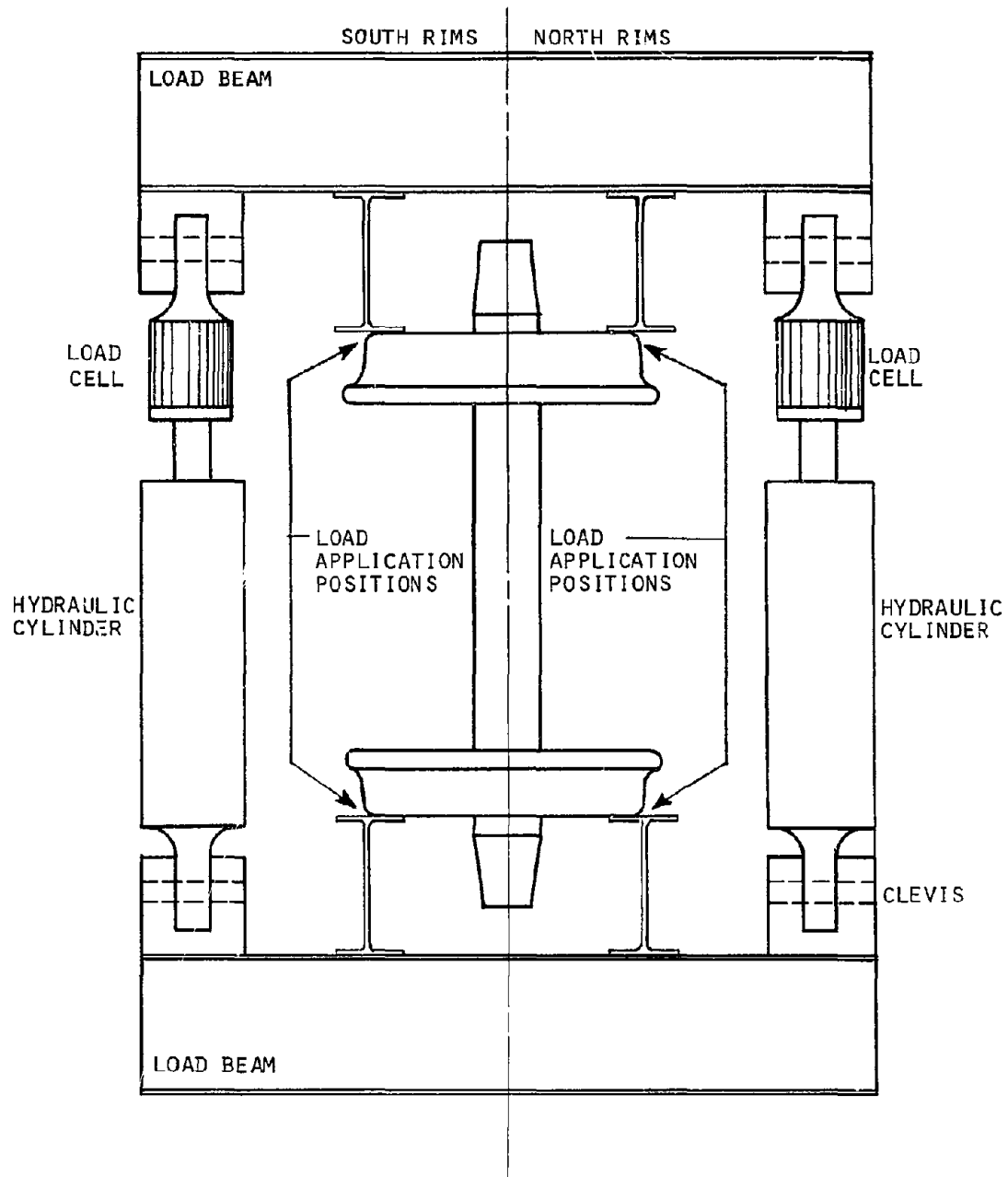


FIGURE 21. LOAD APPLICATION PROCEDURE FOR WHEEL
 PLATE FATIGUE TEST FIXTURE

of 100,000 lb capacity, which are connected to the load frame on either side of the wheel-axle set. By properly balancing the loads acting on each cylinder the resulting load can be directed through one side of the wheel or the other. The fixture was designed and the tests carried out at the Research and Test Laboratory of the Southern Railway System in Alexandria, Virginia. The fixture is illustrated in Figure 22. When alternating loads are applied to the load fixture, the highest stresses are developed in the hub fillet region of the plate. It is here that the development of plate cracks would be anticipated.

5.2.2 Test Procedures and Results - The results of the tests are summarized in Table 5. The first column gives the test number and describes the wheel. The second column indicates the lateral loads which were applied alternately to the north rims and the south rims (see Figure 21) of the wheels. The third column gives the number of cycles of the load. The fourth column shows the strain range for the radial direction on the outside hub fillet. Stresses were determined by strain gages mounted on the wheel. The fifth column indicates the radial stresses derived from the strain readings. About 8 percent of the radial stress results from the tangential stress which accompanies the load. The sixth column presents the equivalent alternating stress for a fully reversed stress cycle. This value is calculated with the assumption that the equivalent of various stress ranges can be related by a Goodman diagram and that the ultimate strength of the wheel plate is 110 ksi.

The first tests were conducted on a pair of wrought steel 36 inch diameter wheels. The test was used to determine the approximate load range where plate cracks would be initiated. The loads in the cylinders were controlled to apply a load of 48,000 lbs to the north rims followed by the removal of this load and the application of a 27,000 lb load to the south rims. After the application of 1,570,000 cycles the programmed load was changed to 40,000 lbs on both rims. This cyclic load was applied until a total of 2,000,000 cycles was exceeded. The rate of load application was approximately 0.5 cycles/sec. No cracks were developed.

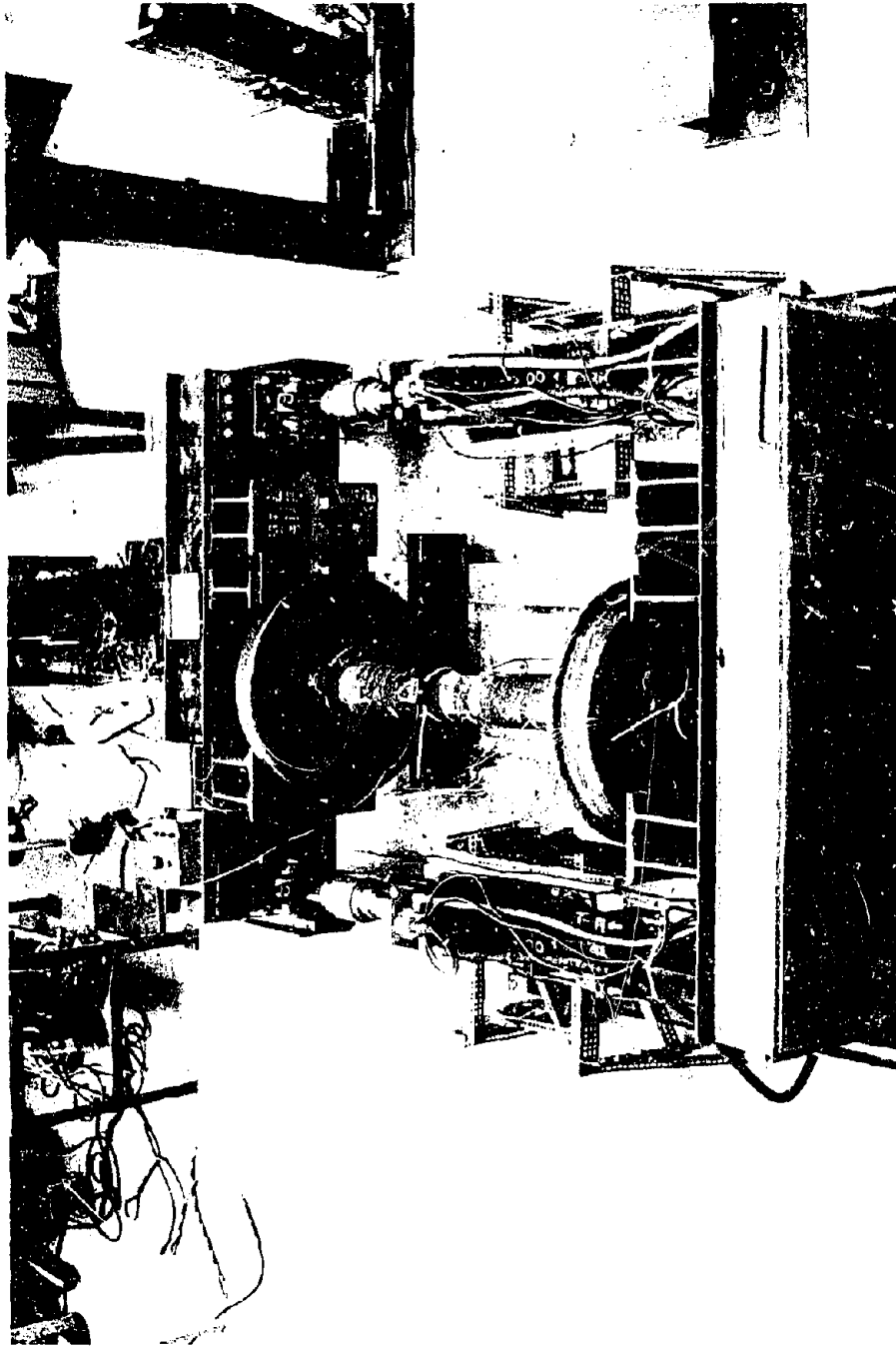


FIGURE 22. WHEEL PLATE FATIGUE TEST LOADING FIXTURE

TABLE 5.-SUMMARY OF WHEEL PLATE FATIGUE TESTS

Test	Lateral Loads (1000 lbs)		Number of Cycles	Strain Range (radial, ϵ_{rr}) at Outside Plate Hub Fillet (North Side) (μ inch/inch)	Stress Range (radial, σ_{rr}) at Outside Plate Hub Fillet (North Side) (1000 psi)	Equivalent σ_{rr} Alternating Stress for Full Reversal (R = -1) (North Side) (1000 psi)
	North Rim	South Rim				
1 (36 inch diam)	48	27	1,570,000	+ 855 - 188	+ 29.4 - 6.5	\pm 20.0
	40	40	442,000	+ 693 - 279	+ 23.8 - 9.6	\pm 17.9
2	80	80	Wheels moved in on axle.			
3 (36 inch diam H36 Class C)	75	44	153,000	+1652 - 521	+ 56.7 - 17.9	\pm 45.3
	84	0	24,000	+1895 0	+ 65.0 0	\pm 46.1
	100	55	100,000	+2256 - 651	+ 77.4 - 22.3	\pm 66.5
	133	58	4,000	+3143 - 697	+107.9 - 23.9	\pm 106.6
4 (28 inch diam B28 Class B)	60	40	750,000	+ 720 - 170	+ 24.7 - 5.8	\pm 16.7
	90	50	500,000	+1080 - 212	+ 37.1 - 7.3	\pm 25.7
	90	10	500,000	+1080 - 43	+ 37.1 - 1.5	\pm 23.0
5 (36 inch diam H36 Class C)	77	40	800,000	+1737 - 481	+ 59.6 - 16.5	\pm 47.3

The results from the first test indicated that the load range would have to be increased if plate cracks were to be initiated. The load range was increased to 80,000 lbs on each rim. The immediate result was that the wheels walked in on the axle. This revealed a limitation in the use of this test fixture for the development of alternating plate stresses. A series of tests were then conducted to determine the maximum load which could be applied to the wheel without having the wheels move in on the axle.

It was determined that if the load was kept below 58,000 lbs on one side of the wheel the initial position of the wheels could be maintained.

The third test series was conducted with 36 inch diameter, H36, Class C wheels. As indicated in Table 5 the tests were begun with an alternating load of 75,000 lbs on the north rims and 44,000 lbs on the south rims. After 153,000 cycles this was changed to 84,000 lbs on the north rims and an additional 24,000 cycles were applied. There was no evidence of crack initiation. The loads were then increased to 100,000 lbs on the north rims and 55,000 lbs on the south rims; 100,000 cycles of this load produced no evidence of wheel failure. As this load range exceeded the initially designed load capacity of the frame, numerous cracks developed in the welds connecting the various structural members of the fixture and these had to be repaired. A final attempt to fail the wheel was made by increasing the load on the north rims to 133,000 lbs and 58,000 lbs on the south rims. This load caused a large amount of distortion due to the bending of the axle. The stroke required to produce the alternating load was over 2 inches and the period of the load cycle was 7 seconds. Strains measured under this loading showed that the yield point was exceeded in the outside plate hub fillet since the strain gage readings indicated a permanent set. The readings eventually stabilized showing that cyclic strain hardening had taken place. The distortion of the axle and the marginal ability of the fixture to carry these loads raised the possibility of a failure which would severely damage the loading cylinders. Consequently this load sequence was terminated after 4000 cycles. Again there was no evidence of crack initiation.

The fourth test series was conducted with 28 inch diameter Class B wrought steel wheels of B28 configuration. These wheels were tested because service experience indicated that plate crack development in these wheels was more likely than in the 36 inch diameter H36 wheels. There was no indication of failure following 750,000 cycles of an alternating load consisting of 60,000 lbs applied to the north rims and 40,000 lbs applied to the south rims.

The load levels were increased to 90,000 lbs on the north rims and 50,000 lbs on the south rims. After 500,000 cycles of this load the axle failed. The wheels were pressed on a new axle and an additional 500,000 cycles of a 90,000 lb load on the north rims and 10,000 lbs on the south rims were applied without any indication of failure.

The fifth test series was conducted with 36 inch diameter Class C wrought steel wheels. This time three V-grooves were chiseled into the plate in an attempt to initiate a crack. The grooves were oriented in the circumferential direction in the vicinity of the outside hub fillet at radial distances of 7-1/2, 8-1/8, and 8-3/4 inches from the centerline of the wheel. The V-grooves were approximately 1/32 inch deep and 1 inch long. The loading sequence consisted of 77,000 lbs on the north rims and 40,000 lbs on the south rims; 800,000 cycles of the load were applied without any indication of crack initiation at the V-grooves. The test was discontinued at this point because excessive deflection in the axle indicated it was near the point of failure.

5.2.3 Interpretation of Wheel Plate Fatigue Tests - The tests revealed a higher tolerance in resisting fatigue damage than had been anticipated. The preliminary test which was conducted at an approximate ± 20 ksi maximum alternating stress level was below the fatigue limit. Bruner's test results (Ref. 9) had indicated a fatigue limit of ± 22.5 ksi on wheel plate materials, but this result was obtained on a rolled finish surface whereas plate surfaces of the wheels used in this test were machined. Therefore, it would have required a rather severe stress concentration feature to initiate the crack within 2,000,000 cycles.

The failure to develop fatigue cracks during the third test series is somewhat surprising. The anticipated fatigue limit (for fully reversed stresses) for the wheel plate material is approximately 44 ksi. An alternating stress level of 55 ksi would be expected to produce visible fatigue damage at 100,000 cycles. Therefore, the initiation of a fatigue crack would have been anticipated during the third loading block where 100,000 cycles

at an equivalent alternating stress of ± 66.5 ksi were applied. The failure of fatigue damage to be produced during the fourth loading block is also surprising. Even though only 4000 cycles were applied, the peak stresses were near the ultimate strength of the material where failure usually occurs within a relatively small number of cycles. The strain gages indicated that permanent set had occurred during this loading.

The test conducted on the 28 inch diameter wheels during the fourth test series resulted in a relatively low alternating stress level because of the thicker plate section on this wheel and the shorter moment arm from the point of load application to the hub plate fillet. It was believed that the higher stress concentration associated with the plate finish on this wheel could lead to crack initiation, but this did not occur. The 90,000 lb lateral load used on the north rims in this test was the maximum load that could be applied with the loading fixture.

The fifth test series resulted in another surprise with the failure of the 800,000 cycle load to initiate a fatigue crack. The only explanation of this result is that the manner in which the V-grooves were placed in the wheel introduced residual compressive stresses at the base of the groove which prevented the stress concentration feature of the groove from initiating the crack.

One can conclude from these tests that the wheel plate design is quite conservative with respect to the development of fatigue cracks due to mechanical loads. The maximum anticipated steady load acting against the flange on sharp curves is approximately 15,000 lbs (Figure 4) which is a relatively low load in terms of the cyclic loads developed during the test program. This indicates that the development of plate cracks is probably associated in some way with the thermal strains from tread braking since these strains are of much higher magnitude. Interaction with or modification of the residual stress field may also be a factor in the development of these cracks.

6. CONCLUSIONS AND RECOMMENDATIONS

The fatigue analyses of truck castings revealed that these components are conservatively designed for the loads normally encountered in service. This conclusion holds provided that the components are not subjected to extremely high load situations and that an adequate standard for the quality of the product is maintained. Under normal circumstances the maximum fluctuating stresses within the truck components should be within the *fatigue limit* so that there would be no accumulation of fatigue damage during the life of the component.

The maximum effective design stresses permitted in truck bolsters are slightly higher than the maximum design stresses permitted in side frames. This may account for the higher failure rate with truck bolsters as compared with side frames (see Subsection 1.2.2). However, this may also be related to improved designs which result from the existence of an AAR fatigue test specification for side frames whereas there is no such requirement for truck bolsters.

The fatigue analyses for evaluating truck castings utilized first-order fatigue calculational procedures. The use of more advanced procedures is not warranted at this time because of the lack of data defining the circumstances under which the high load environment occurs, the variability of the stress fields within these structures and the characteristics of defects or discontinuities within the castings where cracks may be initiated.

Although the designs appear to be adequate under normal conditions it is recognized that fatigue failures do occur. The circumstances under which such failures occur are not adequately defined and therefore the reasons why the apparent design adequacy fails to prevent all fatigue failures cannot be established or ascertained. From the low failure rates encountered it is obvious that when failure occurs one is dealing with extreme values in the statistical sense whether it be with the loads imposed, the strength of the components, or a combination of these factors.

Therefore, one must look at the specific sets of factors leading to failure in order to understand the reasons why failures occur. For example, one recent fatigue failure of a truck bolster resulted from the attachment of a shelf to the spring seat so that the bolster could be used in a higher capacity truck than the one for which it was designed, an obvious misuse of the component. A broader data base describing the detailed circumstances associated with many such failures is required before one can determine the relation of structural adequacy to the present rate of occurrence of these failures.

The severe truck load bounce data presented in Subsection 2.2.3 provides one set of circumstances which might possibly lead to fatigue failure of truck castings. The fatigue calculations made with these data indicate an expected finite life for both the side frame and truck bolster castings. The reasons for the development of the particularly severe loads encountered in this limited set of data are not fully understood, but they are probably associated with the operation of trains at moderately high speeds on relatively rough track. This points out the need to continuously review the structural adequacy and safety implications of the operation of trains under worsening track conditions particularly under the current economic constraints when many railroads find it necessary to defer track maintenance.

The severe load data also raise questions on the basis for the present FRA safety standards for track. These standards set allowable operational speeds on the basis of various track geometric tolerances in gage, alignment, profile and the condition of ties and other elements in the track structure. A more fundamental factor would be a measure of damaging effects on both the track structure and the cars caused by the vibrational excitations of the vehicle suspension system. The damaging effects would be measured by the intensity of the wheel/rail forces and the forces internal to the structure of the car. Allowable speeds could then be established on the basis of track-vehicle interaction forces.

The fatigue analysis of wheels was limited to a review of the factors which lead to plate crack and thermal crack initiation and development. It was shown that plate crack propagation is highly dependent on the state of residual stresses in the hub and rim plate fillet regions. Unfortunately there is not an adequate knowledge of residual stress states of wheels in service. In particular, the possibility of the development of a thin surface layer of compressive stresses in the plate fillets following severe brake heating needs further examination, since this could tend to inhibit plate crack growth. The role of thermal stresses associated with regular service brake applications also needs to be examined further.

The development of thermal cracks is influenced by residual circumferential tensile stresses in the rim, the fluctuating stresses associated with wheel-rail contact zone phenomena, and possibly the thermal stresses in the rim associated with a normal tread brake application. Analytical predictions have been made recently of residual tensile stress changes in wheels. Experimental confirmation of this phenomenon still must be demonstrated. Stress data for the other two phenomena are either not available or not in the proper form for crack growth analysis.

One of the objectives of the test work conducted under this project was to evaluate methods for conducting fatigue tests of wheels. Further study should be given to the development of suitable loading procedures and fixtures for the study of wheel plate fatigue. The loading procedure which was developed under this program has limitations which would preclude its future use in wheel plate fatigue studies. The primary limitation is that the wheel plate appears to be stronger from a fatigue standpoint than the axle so that the axle will fail before the wheel. Also, taking the load between the wheels as a bending moment in the axle leads to a rather large deflection which slows down the rate of load application.

Finally efforts to determine the circumstances under which cracks are initiated and propagated in truck components should be continued because this knowledge would permit a more rational

approach to the definition of freight car safety standards. Frequencies of inspection for these components could be established so that the probability of fatigue failure between inspections would be a minimum.

As a result of the work performed under this project the following specific recommendations can be made.

- a) Conduct additional service load measurement tests to determine the conditions under which abnormally high truck component loads are established. The high loads are the most significant with regard to the accumulation of fatigue damage and circumstances under which these loads occur must be understood.
- b) Develop an information reporting system that will provide the specific details surrounding truck component failures.
- c) Continue the development of test procedures to identify the significant parameters associated with plate and thermal crack propagation in wheels.
- d) Obtain additional data on the stress fields within truck castings, discontinuities where cracks can be initiated and crack growth properties of the materials so that more specific fatigue analyses can be performed.
- e) Evaluate the feasibility of placing operational restrictions on railroad cars so that the probability is reduced of developing truck component loads high enough to lead to failure.

7. REFERENCES

1. Johnson, M. R., "Analysis of Railroad Car Truck and Wheel Fatigue, Part 1, Service Load Data and Procedures for the Development of Fatigue Performance Criteria," Federal Railroad Administration Report FRA-OR&D-75-68, May 1975.
2. "Accident Bulletin, Summary and Analysis of Accidents on Railroads in the United States," Numbers 134-143, U.S. Department of Transportation, Federal Railroad Administration, Office of Safety, various years.
3. "Statistics of Railroads of Class I," 59th Statistical Summary Number, Association of American Railroads, July 1975.
4. "Railroad Freight Car Safety Standards", U.S. Department of Transportation, Federal Railroad Administration, Office of Safety, Title 49-Transportation, Part 215, June 1975.
5. Johnson, M. R., "Effects of Longitudinal Impact Forces on Freight Car Truck Bolsters," Federal Railroad Administration, Report FRA-OR&D-75-10, September 1974.
6. "Wheel and Axle Manual," Association of American Railroads, Mechanical Division, 9th edition, January 1968, p 107.
7. Carter, C. S. and Caton, R. G., "Fracture Resistance of Railroad Wheels," Federal Railroad Administration Report FRA-OR&D-75-12, September 1974.
8. Bruner, J. P., Jones, R. D., Levy, S. and Wandrisco, J. M.; "Effect of Design Variation on Service Stresses in Railroad Wheels," ASME Technical Paper 67-WA/RR-6, November 1967.
9. Bruner, J. P., Benjamin, G. N. and Bench, D. M.; "Analysis of Residual, Thermal, and Loading Stresses in a B33 Wheel and Their Relationship to Fatigue Damage," ASME Journal of Engineering for Industry, May 1967, pp 249-258.
10. Wandrisco, J. M. and Dewez, F. J. Jr., "Study of the Defects that Originate and Develop in the Treads of Railroad Wheels During Service," ASME Paper 60-RR-1, April 1960.
11. "Manual of Standards and Recommended Practices," Section A, Specification for Materials, Specification M201, Steel Castings, Association of American Railroads, Mechanical Division (1971).
12. "Manual of Standards and Recommended Practices," Section A, Specification for Materials, Specification M203, Truck Side Frames, Cast Steel, Association of American Railroads, Mechanical Division (1971).

13. "Manual of Standards and Recommended Practices," Section A, Specification for Materials, Specification M202, Truck Bolsters, Association of American Railroads, Mechanical Division (1971).
14. "Manual of Standards and Recommended Practices," Section A Specifications for Materials, Specification M107, Wheels, Wrought Carbon Steel, Association of American Railroads, Mechanical Division (1972).
15. "Manual of Standards and Recommended Practices," Section A, Specification for Materials, Specification M208, Wheels, Cast Carbon Steel, Association of American Railroads, Mechanical Division (1971).
16. "Manual of Standards and Recommended Practices," Section G, Wheels, Association of American Railroads, Mechanical Division (1972).
17. Johnson, M. R., Welch, R. E., and Yeung, K. S.; "Analysis of Thermal Stress and Railroad Stress Changes in Railroad Wheels Caused by Severe Drag Braking," ASME Technical Paper 75-WA/RT-3, December 1975.
18. Caton, R. G., Guthrie, J. L. and Carter, C. S.; "Fracture Resistance and Fatigue Crack Growth Characteristics of Railroad wheels and Axles," Report No. FRA-OR&D-75-12, September 1974.
19. Stone, D. H., "Residual Stresses in the Plate Fillets of Twenty-Eight-Inch Diameter Wrought Steel Wheels," AAR Research and Test Department Report R-158, May 1974.
20. Wetenkamp, H. R., Sidebottom, O. M. and Schrader, H. J., "The Effect of Brake Shoe Action on Thermal Cracking and on Failure of Wrought Steel Railway Car Wheels," University of Illinois Bulletin 47(77), (Series 387), June 1950.
21. Evans, R. A. and Johnson, M. R., "Analysis of Environmental Truck Component Load and Bolster Fatigue Test Data," AAR Research & Test Report R-246, September 1976.

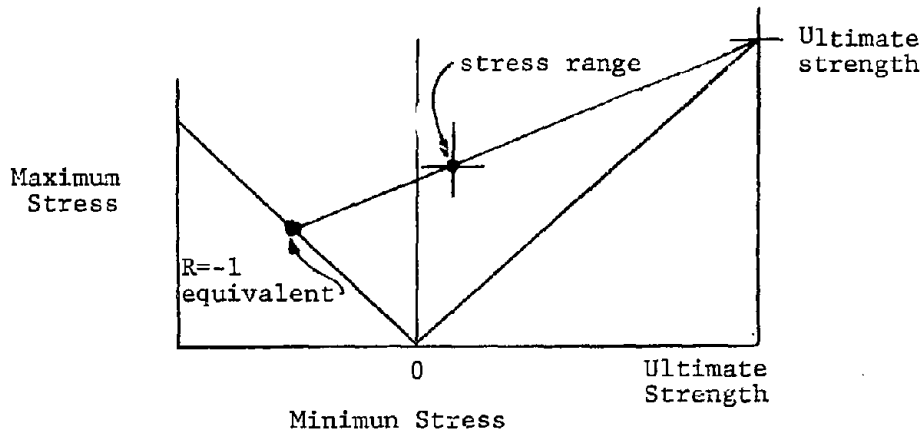
APPENDIX A

CALCULATION OF SIDE FRAME AND TRUCK BOLSTER FATIGUE DATA

The calculations used to derive the fatigue data presented in Section 3.1 of this report are presented in this appendix.

A.1 Calculation of Equivalent Alternating Stress (R=-1) for Side Frame with Peak Load of 120,000 lb

A stress of 8.0 ksi is assumed associated with static load of 60,000 lb (page 24). The stress range for a zero to 120,000 lb load range is then zero to 16.0 ksi. This stress range may be converted to an equivalent (for fatigue) fully alternating stress range (R=-1) through the use of a Goodman diagram:



$$\sigma_a = \frac{\sigma_u (\sigma_{\max} - \sigma_{\min})}{2\sigma_u - (\sigma_{\max} + \sigma_{\min})} \quad (A.1)$$

where

- σ_a is one-half the R=-1 stress range
- σ_u is the ultimate strength (assumed 70 ksi for Grade B steel)
- σ_{\max} is the stress range maximum
- σ_{\min} is the stress range minimum

therefore

$$\sigma_a = \frac{70(16)}{140-16} = \pm 9.03 \text{ ksi}$$

The fatigue limit for Grade B steel is assumed 23 ksi. The minimum anticipated K_f factor to produce fatigue damage is then:

$$K_{fmin} = \frac{23}{9.03} = 2.55$$

A.2 Calculation of Equivalent Alternating Stress (R=-1)
for Side Frame with Peak Load of 200,000 lb
(Tank Car Test Data, Figure 6)

This calculation is similar to the above A.1 calculation. The stress range for a 0-200,000 lb load range is zero to 26.7 ksi. Using Eq. (A.1)

$$\sigma_a = \frac{70(26.7)}{140-26.7} = \pm 16.5 \text{ ksi}$$

The minimum anticipated K_f factor to produce fatigue damage is then:

$$K_{fmin} = \frac{23}{16.5} = 1.39$$

A.3 Calculation of Expected Fatigue Life of Side
Frame and Bolster Castings Using Severe
Load Environmental Data (Figure 15)

The equivalent alternating stress ranges (R=-1) for four ranges of side frame vertical load are shown in Table A.1. The rates of occurrence of these load ranges are also indicated.

Assume the linear damage law to calculate fatigue life for different K_f factors. Assume fatigue properties of Figure 10.

$K_f = 1.75$: only the first load level will cause fatigue damage.

$$1.75 \times 16.5 = \pm 28.9 \text{ ksi}$$

fatigue life (Fig. 10); 900,000 cycles

anticipated service life:

$$\frac{900,000}{0.2} = 4.5 \times 10^6 \text{ miles}$$

Table A.1

Load Level	Step Load Representation of 45-60 mph Side Frame Load Spectrum (Fig. 6) (exceedings/mile)	Load Range (1000 lbs)	Estimated Side Frame Stress Range* (ksi)	Equivalent Alternating Stress for Full Reversal (R=-1) (from Eq. A.1) (ksi)
1	0.2	0-200	0-26.7	± 16.5
2	0.8	8-180	1.1-24.0	± 13.9
3	2.9	14-140	2.1-18.7	± 9.7
4	27	28-100	3.7-13.3	± 5.5

*Based on 8.0 ksi from vertical load of 60,000 lb

$K_f = 2.0$: the first two load levels will cause fatigue damage.

$$2 \times 16.5 = \pm 33 \text{ ksi}$$

fatigue life 400,000 cycles

$$2 \times 13.9 = \pm 27.8 \text{ ksi}$$

fatigue life 1,100,000 cycles

total fatigue damage per mile

$$\frac{0.2}{400,000} + \frac{0.8}{1,100,000} = 0.0000012$$

anticipated service life (inverse of above)

815,000 miles

$K_f = 2.25$: the first two load levels will cause fatigue damage.

$$2.25 \times 16.5 = \pm 37.1 \text{ ksi}$$

fatigue life 170,000 cycles

$$2.25 \times 13.9 = \pm 31.3 \text{ ksi}$$

fatigue life 560,000 cycles

total fatigue damage per mile

$$\frac{0.2}{170,000} + \frac{0.8}{560,000} = 0.0000026$$

anticipated service life (inverse of above)

384,000 miles

$K_f = 2.5$: the first three load levels will cause fatigue damage.

$$2.5 \times 16.5 = \pm 41.3 \text{ ksi}$$

fatigue life 71,000 cycles

$$2.5 \times 13.9 = \pm 34.8 \text{ ksi}$$

fatigue life 282,000 cycles

$$2.5 \times 9.7 = \pm 24.3 \text{ ksi}$$

fatigue life 9,000,000 cycles

total fatigue damage per mile

$$\frac{0.2}{71,000} + \frac{0.8}{282,000} + \frac{2.9}{9,000,000} = 0.0000060$$

anticipated service life (inverse of above)

167,000 miles

$K_f = 3.0$: the first three load levels will cause fatigue damage.
 $3 \times 16.5 = \pm 49.5$ ksi
 fatigue life 10,000 cycles
 $3 \times 13.9 = \pm 41.7$ ksi
 fatigue life 63,000 cycles
 $3 \times 9.7 = \pm 29.1$ ksi
 fatigue life 900,000 cycles
 total fatigue damage per mile
 $\frac{0.2}{10,000} + \frac{0.8}{63,000} + \frac{2.9}{900,000} = 0.000036$
 anticipated service life (inverse of above)
 28,000 miles

The equivalent alternating stress ranges ($R=-1$) for the ranges of bolster vertical bounce load are shown in Table A.2. The rates of occurrence of these load ranges are also indicated.

$K_f = 1.75$: the first two load levels will cause fatigue damage.
 $1.75 \times 18.1 = \pm 31.7$ ksi
 fatigue life 560,000 cycles
 $1.75 \times 15.4 = \pm 27.0$ ksi
 fatigue life 1,100,000 cycles
 total fatigue damage per mile
 $\frac{0.3}{560,000} + \frac{1.7}{1,100,000} = 0.0000021$
 anticipated service life (inverse of above)
 480,000 miles

$K_f = 2.0$: the first two load levels will cause fatigue damage.
 $2 \times 18.1 = \pm 36.2$ ksi
 fatigue life 220,000 cycles
 $2 \times 15.4 = \pm 30.8$ ksi
 fatigue life 630,000 cycles
 total fatigue damage per mile
 $\frac{0.3}{220,000} + \frac{1.7}{630,000} = 0.0000041$
 anticipated service life (inverse of above)
 246,000 miles

Table A.2

Load Level	Step Load Representation of 45-60 mph Bounce Load Spectrum (Fig. 7) (exceedings/mile)	Load Range (1000 lbs)	Estimated Bolster Stress Range* (ksi)	Equivalent Alternating Stress for Full Reversal (R=-1) (from Eq. A.1) (ksi)
1	0.3	0-360	0-28.8	± 18.1
2	1.7	24-330	1.9-26.4	± 15.4
3	8.0	54-210	4.3-16.8	± 7.4

*Based on 9.2 ksi from vertical center plate load of 115,000 lb

$K_f = 2.25$: the first two load levels will cause fatigue damage.

$$2.25 \times 18.1 = \pm 40.7 \text{ ksi}$$

fatigue life 80,000 cycles

$$2.25 \times 15.4 = \pm 34.7 \text{ ksi}$$

fatigue life 280,000 cycles

total fatigue damage per mile

$$\frac{0.3}{80,000} + \frac{1.7}{280,000} = 0.0000098$$

anticipated service life (inverse of above)

102,000 miles

$K_f = 2.5$: the first two load levels will cause fatigue damage.

$$2.5 \times 18.1 = \pm 45.3 \text{ ksi}$$

fatigue life 29,000 cycles

$$2.5 \times 15.4 = \pm 38.5 \text{ ksi}$$

fatigue life 120,000 cycles

total fatigue damage per mile

$$\frac{0.3}{29,000} + \frac{1.7}{120,000} = 0.000025$$

anticipated service life (inverse of above)

41,000 miles

$K_f = 3.0$: the first two load levels will cause fatigue damage.

$$3 \times 18.1 = \pm 54.3 \text{ ksi}$$

fatigue life 3,000 cycles

$$3 \times 15.4 = \pm 46.2 \text{ ksi}$$

fatigue life 22,000 cycles

total fatigue damage per mile

$$\frac{0.3}{3,000} + \frac{1.7}{22,000} = 0.00018$$

anticipated service life (inverse of above)

5,600 miles

A.4 Calculation of Expected Life of Side Frame Castings Based on Amplified Levels of Normal Service Load Data

The equivalent alternating stress ranges ($R=-1$) for the 2 and 3σ values of the side frame load spectrum (Figure 3) are given

in Table A.3 for three load ranges. The rates of occurrence of these load ranges are also indicated. Fatigue data are taken from Figure 10.

2 σ load; $K_f = 3.5$:

the first load level will cause fatigue damage.

$$7.7 \times 3.5 = \pm 27 \text{ ksi}$$

fatigue life 1,600,000 cycles

total fatigue damage per mile

$$\frac{.01}{1,600,000} = .63 \times 10^{-8}$$

anticipated service life (inverse of above)

$$1.6 \times 10^8 \text{ miles}$$

2 σ load; $K_f = 4.0$:

the first two load levels will cause fatigue damage.

$$7.7 \times 4 = \pm 30.8 \text{ ksi}$$

fatigue life 630,000 cycles

$$6.6 \times 4 = \pm 26.4 \text{ ksi}$$

fatigue life 2,000,000 cycles

total fatigue damage per mile

$$\frac{0.1}{630,000} + \frac{.09}{2,000,000} = .61 \times 10^{-7}$$

anticipated service life (inverse of above)

$$1.6 \times 10^7 \text{ miles}$$

2 σ load; $K_f = 4.5$:

the first two load levels will cause fatigue damage.

$$7.7 \times 4.5 = \pm 34.7 \text{ ksi}$$

fatigue life 280,000 cycles

$$6.6 \times 4.5 = \pm 29.7 \text{ ksi}$$

fatigue life 740,000 cycles

total fatigue damage per mile

$$\frac{0.01}{280,000} + \frac{0.09}{740,000} = 0.00000016$$

anticipated service life (inverse of above)

$$6,400,000 \text{ miles}$$

Table A.3

Load Level	Step Load Representation of Side Frame Vertical Load Spectrum (Fig. 3) (exceedings/mile)	Load Level Above Average Value	Load Range* (1000 lbs)	Estimated Side Frame Stress Range** (ksi)	Equivalent Alternating Stress for Full Reversal (R=-1) (from Eq. A.1) (ksi)
1	.01	2 σ	16-116	2.1-15.5	+ 7.7
2	.09	2 σ	22-108	2.9-14.4	+ 6.6
3	.90	2 σ	30-96	4.0-12.8	+ 5.0
1	.01	3 σ	10-124	1.3-16.5	+ 8.7
2	.09	3 σ	20-112	2.7-14.9	+ 7.0
3	.90	3 σ	26-100	3.5-13.3	+ 5.6

* Note values in Fig. 3 must be multiplied by 2 for total side frame load.

** Based on 8 ksi for total vertical load of 60,000 lbs.

2σ load; K_f = 5.0:

all three load levels will cause fatigue damage.

$$7.7 \times 5 = \pm 38.5 \text{ ksi}$$

fatigue life 110,000 cycles

$$6.6 \times 5 = \pm 33 \text{ ksi}$$

fatigue life 400,000 cycles

$$5.0 \times 5 = \pm 25.0 \text{ ksi}$$

fatigue life 5,000,000 cycles

total fatigue damage per mile

$$\frac{0.01}{110,000} + \frac{0.09}{400,000} + \frac{0.9}{5,000,000} = 0.00000050$$

anticipated service life (inverse of above)

$$2,000,000 \text{ miles}$$

3σ load, K_f = 3.0:

the first load level will cause fatigue damage.

$$3 \times 8.7 = \pm 26.1 \text{ ksi}$$

fatigue life 2,200,000 cycles

total fatigue damage per mile

$$\frac{0.01}{2,200,000} = .45 \times 10^{-8}$$

anticipated service life (inverse of above)

$$2.2 \times 10^8 \text{ miles}$$

3σ load; K_f = 3.5:

the first two load levels will cause fatigue damage.

$$3.5 \times 8.7 = \pm 30.5 \text{ ksi}$$

fatigue life 630,000 cycles

$$3.5 \times 7.0 = \pm 24.5 \text{ ksi}$$

fatigue life 6,300,000 cycles

total fatigue damage per mile

$$\frac{0.01}{630,000} + \frac{0.09}{6,300,000} = 3.0 \times 10^{-8}$$

anticipated service life (inverse of above)

$$3.3 \times 10^7 \text{ miles}$$

3σ load; K_f = 4.0:

the first two load levels will cause fatigue damage.

$$4 \times 8.7 = \pm 34.8 \text{ ksi}$$

fatigue life 300,000 cycles

$$4 \times 7.0 = \pm 28 \text{ ksi}$$

fatigue life 1,100,000 cycles

total fatigue damage per mile

$$\frac{0.01}{300,000} + \frac{0.09}{1,100,000} = .12 \times 10^{-6}$$

anticipated service life (inverse of above)

$$8.7 \times 10^6 \text{ miles}$$

3σ load; K_f = 4.5:

all three load levels will cause fatigue damage.

$$4.5 \times 8.7 = \pm 39.2 \text{ ksi}$$

fatigue life 110,000 cycles

$$4.5 \times 7.0 = \pm 31.5 \text{ ksi}$$

fatigue life 560,000 cycles

$$4.5 \times 5.6 = \pm 25.2 \text{ ksi}$$

fatigue life 4,000,000 cycles

total fatigue damage per mile

$$\frac{0.01}{110,000} + \frac{0.09}{560,000} + \frac{0.9}{4,000,000} = .48 \times 10^{-6}$$

anticipated service life (inverse of above)

$$2.1 \times 10^6 \text{ miles}$$

3σ load; K_f = 5.0:

all three load levels will cause fatigue damage.

$$5 \times 8.7 = \pm 43.5 \text{ ksi}$$

fatigue life 44,000 cycles

$$5 \times 7.0 = \pm 35 \text{ ksi}$$

fatigue life 260,000 cycles

$$5 \times 5.6 = \pm 28 \text{ ksi}$$

fatigue life 1,000,000 cycles

total fatigue damage per mile

$$\frac{0.1}{44,000} + \frac{0.09}{260,000} + \frac{0.9}{1,000,000} = 1.5 \times 10^{-6}$$

anticipated service life (inverse of above)

$$680,000 \text{ miles}$$

APPENDIX B
REPORT OF INVENTIONS

The work conducted under this program involved performing a detailed fatigue evaluation of freight car truck castings and wheels. The conservative nature of present designs with respect to normal service environments is shown.

After a diligent review of the work performed under this contract no innovation, discovery, improvement, or invention was made.